STUDY OF NEW TRACK STRUCTURE DESIGN

PHASE II

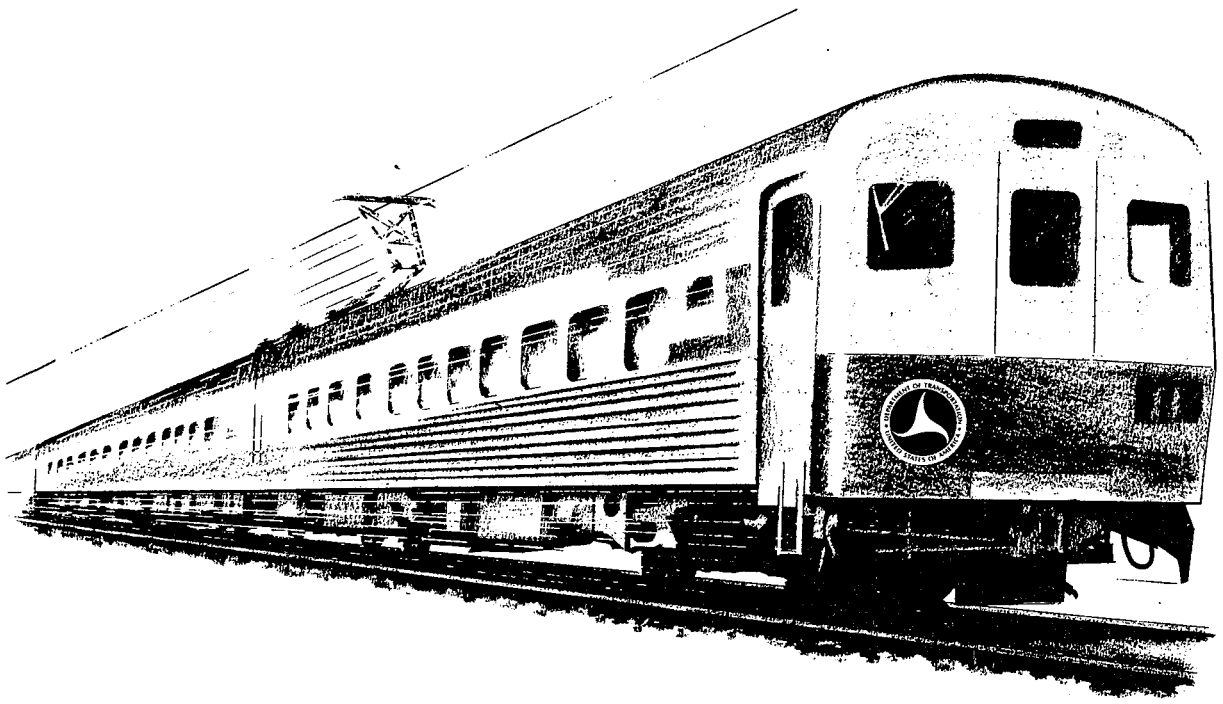

FEDERAL RAILROAD ADMINISTRATION

OFFICE OF HIGH-SPEED GROUND TRANSPORTATION

TECHNICAL REPORT STANDARD TITLE PAGE

1. Report No.	2. Government Accession No.	3. Recipient's Catalog No.
FRA-RT-72-15		

4. Title and Subtitle	5. Report Date
Study of New Track Structure Design Phase II	August 1968
	6. Performing Organization Code

7. Author(s)	8. Performing Organization Report No.
H. C. Meacham, J.E. Voorhees, J. G. Eggert, et al	

9. Performing Organization Name and Address	10. Work Unit No.
Battelle Memorial Institute 505 King Avenue Columbus, Ohio 43201	11. Contract or Grant No.
	13. Type of Report and Period Covered
12. Sponsoring Agency Name and Address	Summary Report
Engineering, Research and Development Division Federal Railroad Administration Washington, D.C. 20591	14. Sponsoring Agency Code

15. Supplementary Notes

16. Abstract

Phase I of this research investigation was undertaken in September, 1966, for the Office of High Speed Ground Transportation (OHSGT) of the Department of Commerce by Battelle Memorial Institute for the purpose of conceiving new and improved track structures for high-speed trains. As a result of the Phase I program, a number of track structures and fasteners were devised which met the specified requirements.

Following the conclusion of the Phase I program, the OHSGT requested additional studies and computer analyses of track structures and rail fasteners. The additional track structures of interest were chosen by OHSGT from many designs which had been submitted to them. In addition to the analysis of the track structures, they were interested in a more detailed analysis of rail fasteners, particularly any analysis which was amendable to computer techniques. This project (which was then designated as Phase II) was then conducted, and the results are summarized in this report.

This report contains detailed discussion of material summarized in: "Studies For Rail Vehicle Track Structures," PB 149 139, and is a reference source sited in that document.

17. Key Words	18. Distribution Statement
Track structure designs, improved track stability, track response computer programs, soil deterioration factor, rail fastenings.	Availability is unlimited. Copies may be purchases from the National Technical Information Service, Springfield, Va. 22151, for $3.00 a copy.

19. Security Classif. (of this report)	20. Security Classif. (of this page)	21. No. of Pages	22. Price

Form DOT F 1700.7 (8-69)

TABLE OF CONTENTS

LIST OF FIGURES

TABLE OF CONTENTS (Cont.)

Page

LIST OF FIGURES (Cont.)

LIST OF TABLES

TABLE OF CONTENTS (Cont.)

Page

LIST OF TABLES (Cont.)

LIST OF SYMBOLS

A_L = Bearing area on subgrade beneath ballast, $in.^2$

A_o = Tie bearing area on ballast, $in.^2$

C_R = Effective damping of lumped parameter model, lb-sec/in.

E_b = Young's modulus of elasticity of ballast, psi

EI_R = Flexural rigidity of rail, $lb\text{-}in.^2$

ΔF_{pr} = Loss of rail fastener preload, lb

f = Track structure natural frequency, cps

K_c = Rail fastener clip vertical spring rate, lb/in.

K_{pt} = Rail pad torsional spring rate, in.-lb/radian

K_u = Upper limit value of clip vertical spring rate, lb/in.

K_v = Total vertical stiffness of rail fastener, lb/in.

k = Rail support spring rate at each tie, lb/in.

k_b = Ballast spring rate, lb/in.

k_{bs} = Series spring rate of ballast and soil, lb/in.

k_o = Soil foundation bulk modulus, $lb/in.^3$

k_p = Pad stiffness, lb/in.

k_R = Overall rail stiffness for point load, lb/in.

k_s = Soil spring rate, lb/in.

k_t = Tie spring rate, lb/in.

L = Ballast depth, in.

L_R = Effective rail length of lumped parameter system model, in.

ℓ_1 = Distance from lateral load to twist center, in.

ℓ_2 = Distance from rail center to clip contact point, in.

ℓ_t = Tie spacing, in.

LIST OF SYMBOLS (Cont.)

m_r = Mass of rail per unit length, lb-sec^2

m_R = Mass of rail for length L_R, lb-sec^2

m_t = Tie mass per inch of rail, lb-sec^2/in.^{2}

P = Static wheel load = 1/8 car weight, lb

P_ℓ = Lateral wheel load, lb

P_v = Vertical load on rail fastener, lb

p_L = Subgrade pressure, psi

p_o = Ballast pressure, psi

w = Width of rail base contacting rail pad, in.

y = Vertical rail deflection relative to fastener, in.

y_o = Rail deflection, in.

y_t = Total vertical clip deflection, in.

y_η = Vertical rail deflection at clip due to angular rotation η, in.

η = Angular deflection of rail cross section, radian

σ_{rail} = Rail bending stress, psi

STUDY OF NEW TRACK STRUCTURE DESIGNS

PHASE II

by

H. C. Meacham, J. E. Voorhees,
G. J. Eggert, and J. J. Enright

INTRODUCTION

Phase I of this research investigation was undertaken in September, 1966, for the Office of High-Speed Ground Transportation (OHSGT) of the Department of Commerce by Battelle Memorial Institute for the purpose of conceiving new and improved track structures for high-speed trains. The need for improved track structures was recognized as being one of the leading technical and economic problems involved with the development of safe, comfortable, high-speed passenger train service.

Specific features to be incorporated in such improved track structures included provisions for accurate leveling and alignment of the rails at the time of construction; long-term dimensional stability and freedom from the requirement for maintenance in spite of heavy, high-speed traffic and various soil conditions; and provisions for positive readjustment of rail alignment and elevation should the need develop. The ground rules under which this program was conducted specified only that the standard railhead contour and gauge should be retained, so that standard rolling stock could operate on all new track systems recommended.

As a result of the Phase I program, a number of track structures and fasteners were devised which met the specified requirements.

Following the conclusion of the Phase I program, the OHSGT requested additional studies and computer analyses of track structures and rail fasteners. The additional track structures of interest were chosen by OHSGT from many designs which had been submitted to them. In addition to the analysis of the track structures, they were interested in a more detailed analysis of rail fasteners, particularly any analysis which was amenable to computer techniques. This project (which was then designated as Phase II) was then conducted, and the results are summarized in this report.

SUMMARY

Eight additional track structures were analyzed using methods previously described in the Phase I report, including both hand calculations and digital and analog computer analyses to determine their functional performance. These structures are shown in Figures 1 through 6. Note that the eight structures ranged from conventional rail supported on wood ties to heavy concrete beam-supported structures such as might be used for elevated construction. The structure shown in Figure 6 was the only one not supported continuously on the subgrade; it was supported periodically on piers. As shown in Figure 5, a continuous beam structure supported by soil was also included, and an evaluation was made to determine the effect of joints in the beams of this otherwise continuous structure. Variations of several of the structures (for example, 21- and 30-inch tie spacing with and without resilient pads for the structure shown in Figure 2) were also analyzed.

The comparison of various structures was made on the basis of their performance under both static and dynamic load. The static load-deflection response is analogous to the response from rolling wheel loads if the track and wheel are perfectly smooth and speeds are low enough to keep roadbed damping loads to a negligible value. Only functional characteristics were considered; economic factors were not considered during this Phase II work.

All of the structures which were supported periodically by ties or their equivalent were compared with each other and with the twin longitudinal beam-type structure, which approaches conventional structures in terms of bearing area per unit length, overall spring rate, etc. This comparison for the case where all the structures are loaded by a 22,500-pound wheel load (45,000-pound axle load) is shown in Table 1. The structures are listed in order of increasing overall spring rate (wheel load divided by rail deflection). In cases where a resilient pad was used on tie-supported structures, its stiffness was approximately 700,000 pounds/inch per pad. For the beam-supported structures, pad stiffness was 750,000 pounds/inch, assuming 30-inch spacing.

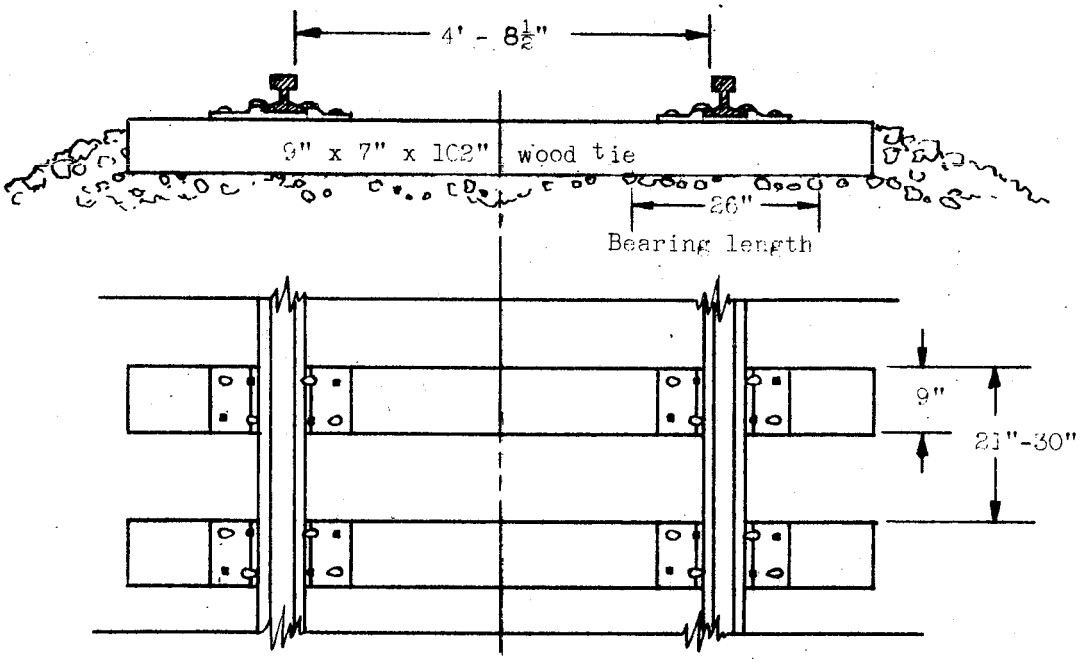

FIGURE 1. CONVENTIONAL TRACK STRUCTURE WITH WOODEN TIES

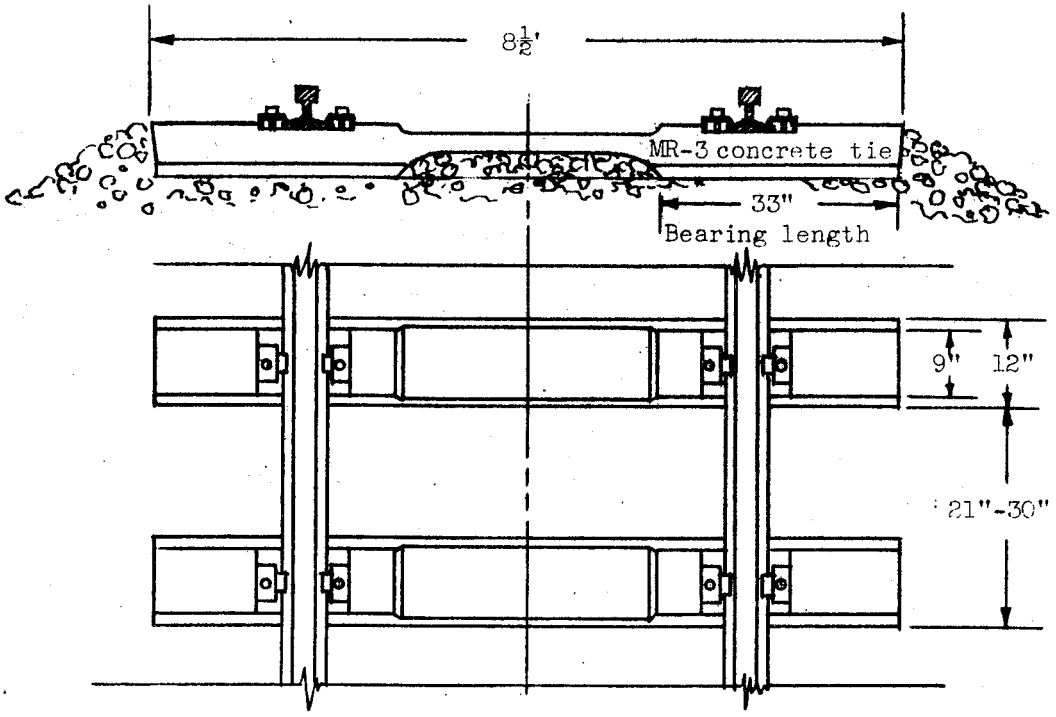

FIGURE 2. CONVENTIONAL TRACK STRUCTURE WITH CONCRETE TIES

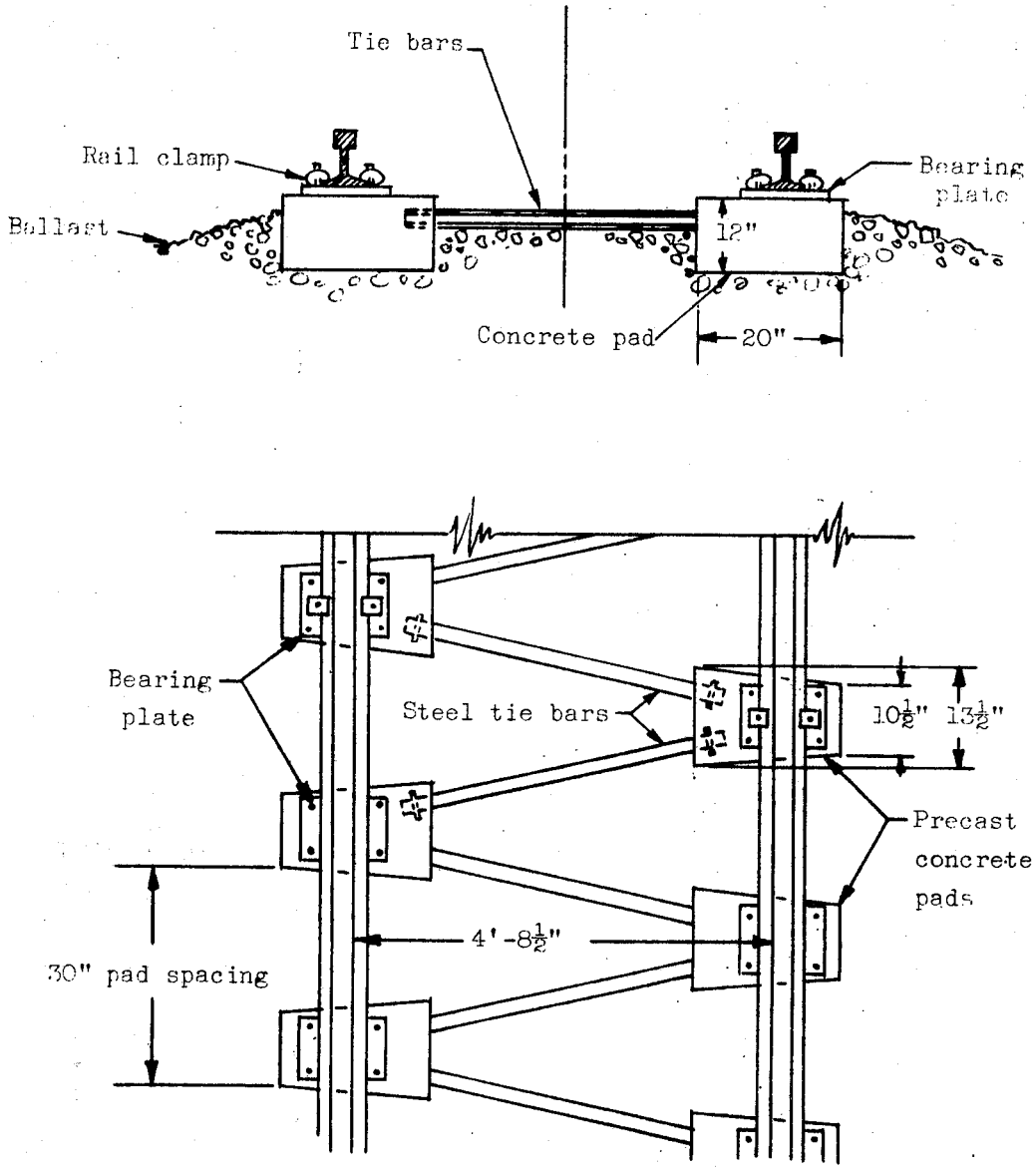

FIGURE 3. DUTCH "ZIG-ZAG" TRACK STRUCTURE

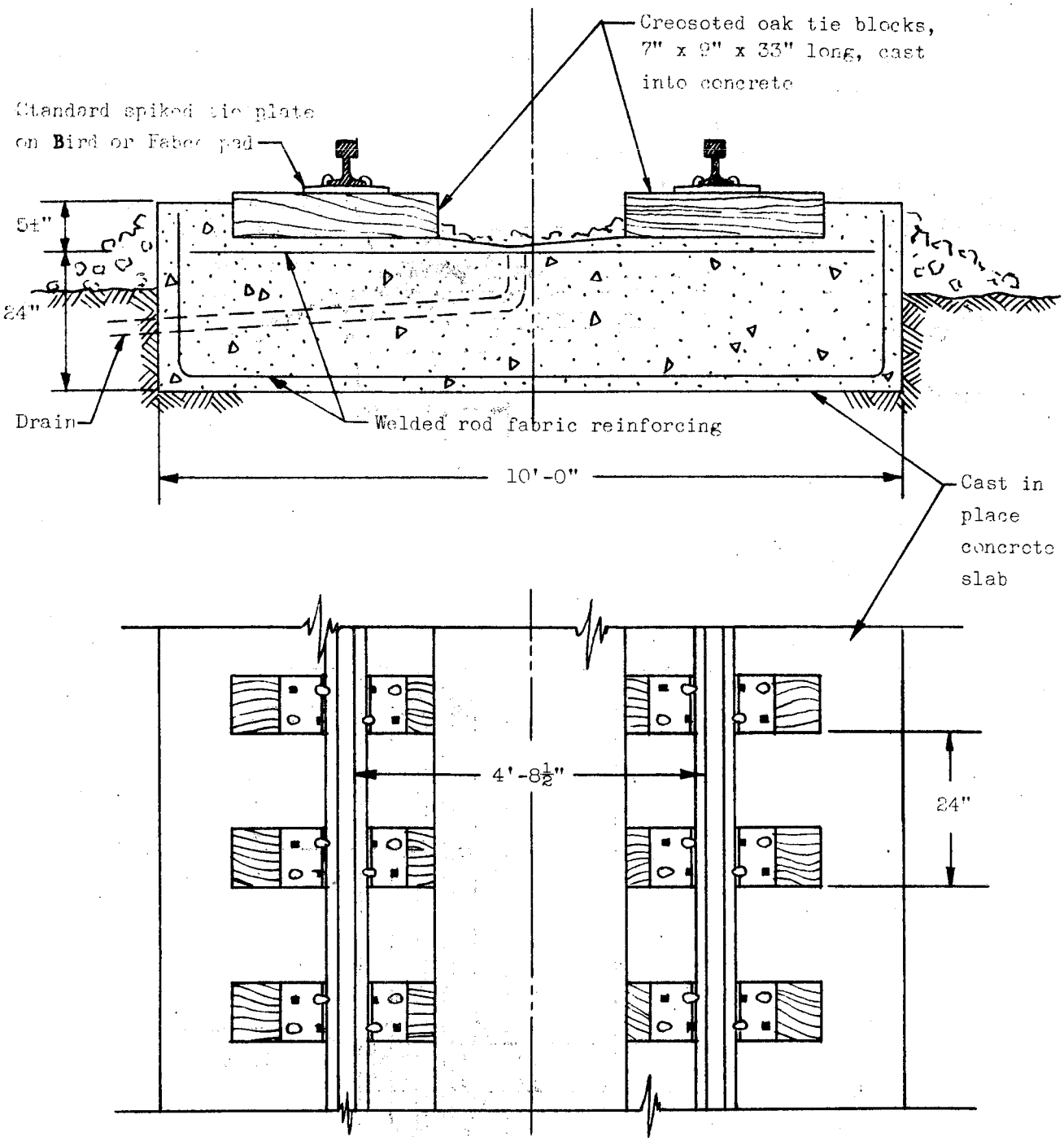

FIGURE 4. STUB-TIES IN CONCRETE SLAB (LOUIS T. KLAUDER NUMBER 1)

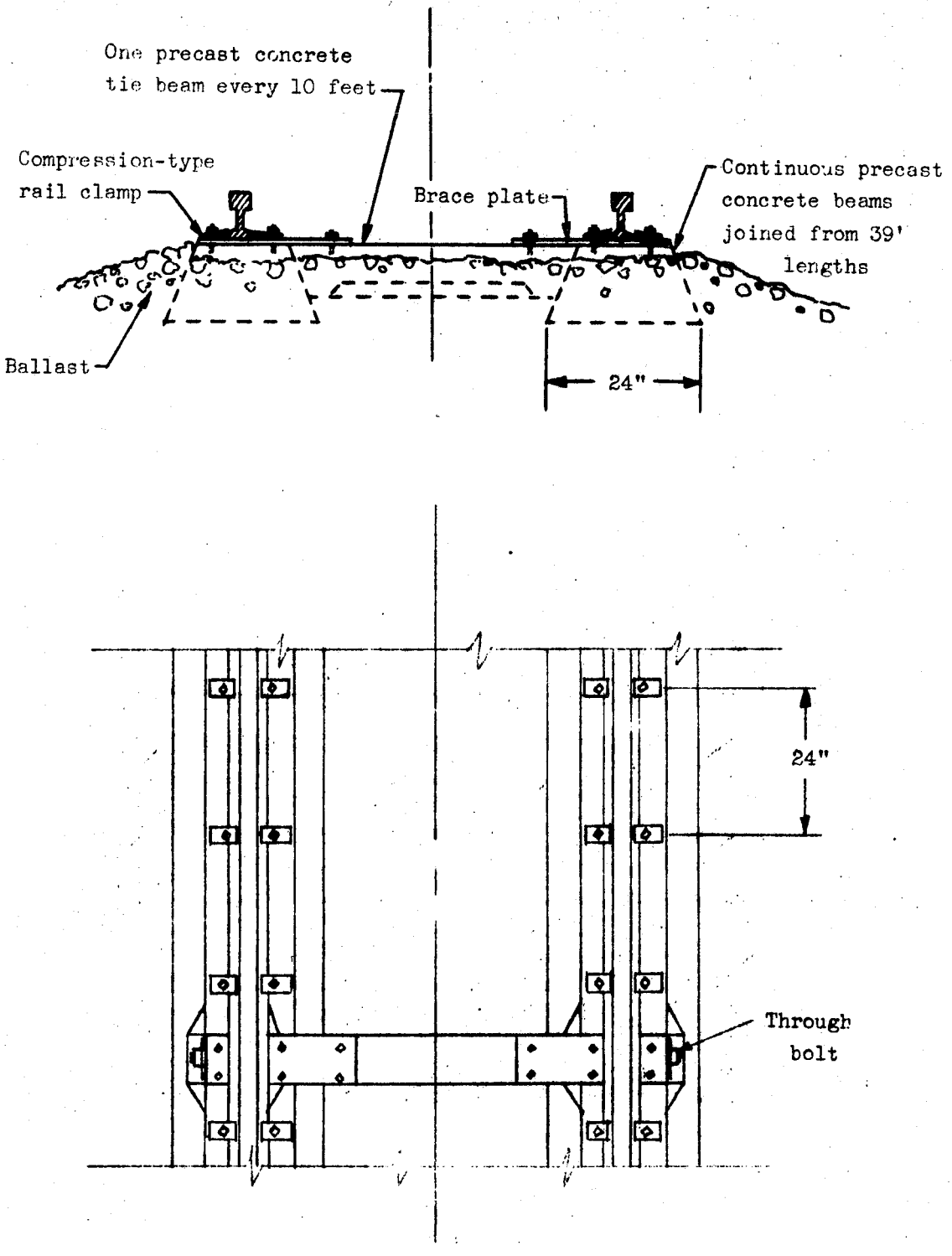

FIGURE 5. TWIN LONGITUDINAL REINFORCED CONCRETE BEAMS (CROSSTIES AT 10-FOOT INTERVALS)

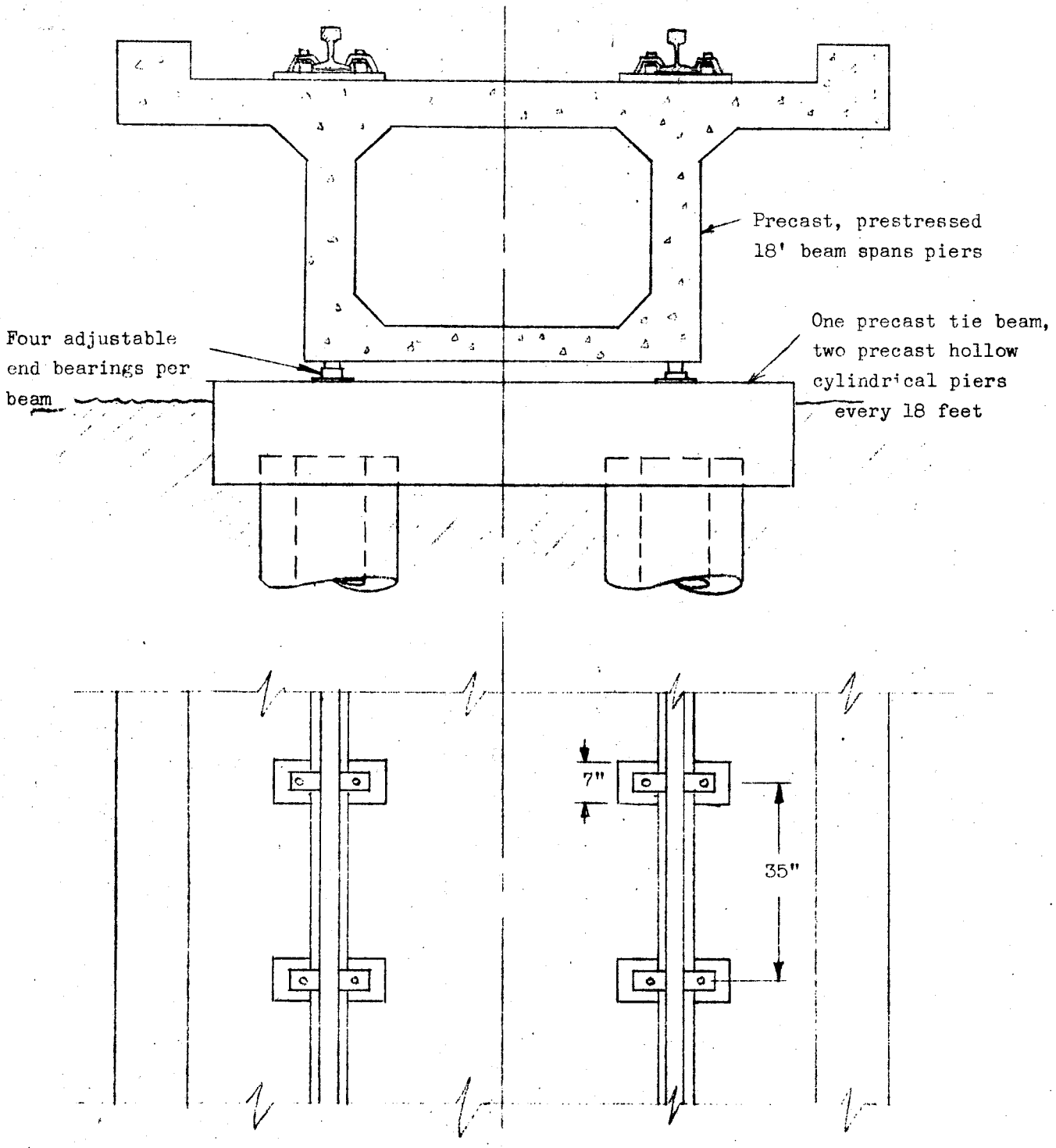

FIGURE 6. CONCRETE BEAM ON PIERS (LOUIS T. KLAUDER NUMBER 8)

TABLE 1. RESPONSE OF SEVERAL TRACK STRUCTURES TO SINGLE AXLE LOAD*

Description	Pad Stiffness, lb/inch	Tie Spacing, inches	Subgrade Modulus, $lb/inch^3$	Overall Stiffness, lb/inch	Tie Bearing Pressure, psi	Rail Bending Stress, psi	Subgrade** Pressure, psi
Dutch Zig-Zag	∞	30	100	168,000	27	10,600	5.9
MR-3 Concrete Ties	700,000	30	100	200,000	17.2	10,100	4.6
MR-3 Concrete Ties	∞	30	100	212,000	17.6	9,800	4.7
9" x 7" x 102" Wood Ties	700,000	21	100	215,000	20.8	10,000	4.2
9" x 7" x 102" Wood Ties	∞	21	100	228,000	21.1	10,000	4.2
MR-3 Concrete Ties	700,000	21	100	263,000	13.0	9,300	3.5
MR-3 Concrete Ties	∞	21	100	280,000	13.4	8,500	3.6
Twin Longitudinal Beams	750,000	Pads at 30	100	314,000	----	6,280	5.85***
MR-3 Concrete Ties	700,000	30	500	415,000	21.4	8,000	5.7
Dutch Zig-Zag	∞	30	500	422,000	35.4	8,100	7.7
9" x 7" x 102" Wood Ties	700,000	21	500	480,000	27.4	6,800	5.4
MR-3 Concrete Ties	∞	30	500	535,000	24.0	6,600	6.4
MR-3 Concrete Ties	700,000	21	500	540,000	16.6	7,300	4.4
9" x 7" x 102" Wood Ties	∞	21	500	562,000	28.8	6,600	5.8
Twin Longitudinal Beams	750,000	Pads at 30	500	640,000	----	6,415	7.5***
MR-3 Concrete Ties	∞	21	500	700,000	18.2	6,300	4.8

* Axle load = 45,000 lb (22,500 lb/wheel), rail weight = 132 lb/yd.

** At base of 24-inch ballast depth.

*** Beam bearing pressure.

One of the first items of interest is the ranking of various structures with regard to overall stiffness. In addition to the obvious effect of the stiffer soil increasing stiffness, the not-so-obvious effect of tie bearing area (per unit length) is primarily responsible for the differences in overall track spring rate. Thus, the concrete-tie track is stiffer than a wood-tie track not because concrete ties themselves are much stiffer than wood ties, but because their bearing area is considerably greater than that of wood ties (assumed to be 50 percent of the total tie area for wood ties, although values as high as 80 percent are sometimes quoted). This results in lower bearing pressures, less deflection, and a correspondingly higher spring rate.

If the data in Table 1 is plotted, it will be found that, in general, the subgrade pressure (24 inches beneath the ties at the ballast-subgrade interface) for a given soil decreases as overall stiffness increases, and rail bending stress decreases as overall stiffness increases. These are desirable trends which tend to favor the stiffer track construction.

Longitudinal beam-type structures, such as the commercially available Liberty track design (39-foot precast beams) or any of several continuous beam designs developed by Battelle in the Phase I report, are quite stiff and show a marked reduction in bearing pressure. Note that for the beam structure listed in Table 1 (continuous reinforced concrete beams having the same cross section as the Liberty track beams were assumed) the bearing pressure directly beneath the beam is nearly as low as that in the subgrade 2 feet beneath the ties for the tie-supported structures. The net result is that the peak roadbed pressure is 10 to 20 psi less than for tie-supported structures. This should result in a much more stable track structure. Another point which should be noted is that for the tie-supported structures calculations are based on the assumption that each tie bears load equally; in practice this condition is rarely achieved for long. For the beam-type structures, calculated pressures are much more likely to be obtained in practice because the beam stiffness minimizes local deflection with the associated load concentration.

Calculations for the more complex structures, including the twin longitudinal beams (with joints at 39-foot intervals) and the pier-supported Klauder Structure No. 8, were made with the aid of a digital computer program, with the loading representing a loaded truck--that is, two adjacent axles each carrying 45,000 pounds. The rail deflections for this case are different (not necessarily greater) than for the single axle loading, since the deflection of each wheel is influenced by the deflection of the adjacent wheel. The response of several track structures under double axle loading is shown in Table 2, again listed in order of overall stiffness to applied wheel loads.

Several facts can be noted from this table. One is that the pier-supported structure is quite soft, even for the case of stiff pier support. Also, rail stresses are high due to the bending of the rail over the piers. Conversely, the slab-type structure is the stiffest, giving low bearing pressures and rail bending stresses. With respect to the twin longitudinal beams, the most interesting result is that joints increase the beam deflections and bearing pressures only slightly. However, the presence of the joint increases the rail bending stress noticeably.

In summary, then, the continuously supported beam-type structures show the desirable attributes of lower bearing pressures and rail stresses, and joints in the beams have a surprisingly small effect. The pier-supported structure compares favorably with the continuously supported structures only if the piers are relatively stiff. The low beam stresses and shape of the deflection curves (see text) indicate that the beams in the pier-supported structure have an excessive bending stiffness, meaning that a smaller (and cheaper) structure would actually be a better one.

The dynamic response of several of the tie-supported track structures was determined from an analog computer simulation, using as inputs sinusoidal and step-type track profiles. Track structures and a Budd 100-ton passenger car were represented by lumped parameter systems. Table 3 shows typical response data for the step-type inputs.

TABLE 2. RESPONSE OF SEVERAL TRACK STRUCTURES TO DOUBLE AXLE LOADS*

Description	Resilient Pad Spacing, inches	Subgrade Modulus, lb/inch^3	Overall Stiffness, lb/inch	Bearing Pressure, psi	Rail Bending Stress, psi	Beam Bending Stress, psi	Beam or Tie Deflection, inches
Klauder No. 8 (Pier-Supported)	30	**	43,300	305.0	11,340	49	0.500
MR-3 Concrete Ties	30	100	196,000	13.4	9,300	--	0.088
Twin Longitudinal Beams (39' Joints)	30	100	204,200	9.8	7,478	282	0.095
Twin Longitudinal Beams (No Joints)	30	100	225,000		5,974	342	0.090
Klauder No. 8 (Pier Supported)	30	***	225,000	320	7,028	48	0.090
MR-3 Concrete Ties	30	500	430,000	16.1	7,350	--	0.041
Klauder No. 1 (Concrete Slab)	30	100	527,000	4.2	7,350	165	0.042
Continuous Longitudinal Beam (No Joints)	30	500	608,000	10.0	5,502	211	0.020
Twin Longitudinal Beams (39' Joints)	30	500	608,000	10.4	6,300	210	0.020
Klauder No. 1 (Concrete Slab)	30	500	2,210,000	5.1	4,140	112	0.010

* Axle Load = 45,000 lb (22,500 lb/wheel); Axle Spacing = 8.5 ft.; Rail Weight = 132 lb/yd; Resilient Pad Stiffness = 750,000 lb/inch.

** Pier Stiffness = 7×10^4 lb/inch.

*** Pier Stiffness = 42×10^4 lb/inch.

TABLE 3 DYNAMIC RESPONSE OF TRACK STRUCTURES TO 1/4-INCH STEP-TYPE PROFILE INPUTS

Structure (See Table 5 for More Complete Description)	Subgrade Modulus, lb/in.^{3}	Overall Stiffness, lb/in.	Car Body Acceleration, in./sec^2 $\ddot{X}_6$	Wheel Overshoot Displacement, in. X_1	Rail Overshoot Displacement, in. Y_1	Peak Wheel-Rail Force, lb $F_{12}/1000$
Wood Ties @21", No Pad	100	228,000	66.4	0.105	0.102	50.4
Wood Ties @21", Resilient Pad	100	215,000	65.0	0.106	0.111	51.6
MR-3 Ties @21", No Pad	100	280,000	68.0	0.088	0.083	60.0
MR-3 Ties @21", Resilient Pad	100	263,000	65.0	0.088	0.087	60.0
Dutch Zig-Zag	100	168,000	52.8	0.083	0.083	84.6*
Wood Ties @21", No Pad	500	562,000	75.2	0.070	0.053	71.4
MR-3 Ties @21", No Pad	500	700,000	76.0	0.062	0.047	78.0
MR-3 Ties @21", Resilient Pad	500	540,000	74.4	0.068	0.060	78.0
Dutch Zig-Zag	500	422,000	73.6	0.079	0.075	72.0

* On all structures the wheel-rail forces went to zero 2X (bounced twice) except Structure 5 on a soft subgrade, which bounced about 8 times.

Plotting the data for dynamic response shows, in general, the following trends:

(1) For step inputs, the peak impact wheel-rail force increases as overall track stiffness increases

(2) For step inputs, car body accelerations increase as overall track stiffness increases

(3) Tie-ballast peak pressures decrease as overall track stiffness increases

(4) For sinusoidal inputs, vehicle-track structure frequency response did not vary appreciably for any of the tie-supported structures except the Dutch "zig-zag" type.

The Dutch "zig-zag" structure proved to be quite an anomaly. Under static load rail stresses, tie-ballast pressures, and soil pressures were the highest, while natural frequency and overall spring rate were the lowest. All of these characteristics can be attributed to the low bearing area per unit length.

The dynamic response of the structure was also unique, giving a lower amplitude of vibration with sinusoidal excitation but higher rail displacements and wheel-rail forces for the step-type input. These characteristics result from the relatively high-mass, low-spring rate characteristics of this dynamic system. In summary, the Dutch "zig-zag" track structure appears to offer no advantages.

With respect to the other tie-supported structures, including variations of tie spacing and use of a stiff resilient pad, dynamic performance differences were minor rather than substantial, with the trends noted above making the choice of overall track stiffness somewhat of a compromise, depending on whether the ballast, wheels and rails, or vehicle are to be favored.

This problem of maintaining a relatively stiff rail-support structure while still minimizing dynamic impact forces on vehicle and track structure, exists both in tie-type and longitudinal beam-type structures--although the

greater stiffness of the beam-type structures makes it potentially more serious for them. Fortunately, this problem can be minimized in either type of structure by the use of resilient pads between the rail and the support, whether it be a tie or a beam.

In addition to their shock isolation function, resilient members may serve three other basic functions:

(1) They act as a load distribution element to provide a good seating surface (minimizing stress concentrations) on the potentially rough concrete beam surface;

(2) They can be designed to electrically insulate the rail from the support structure;

(3) They provide some noise attenuation, the amount being variable, depending upon other design features.

The range of 700,000 to 750,000 pound/inch per pad used in this study was based on two factors. First, in the Phase I study the upper value was chosen as being desirable for use with the massive beam-type structures, and secondly, this value is fairly close to the stiffness of many of the commercial resilient pads now in service both here and abroad. The results of this analysis, however, indicate that softer pads are needed with the tie-type structures to make a significant difference in their performance (as opposed to having no pad). The resiliency of the pad also is important to the characteristics of the rail fastener, as discussed below.

In addition to the analysis of the track structures, the general problem of rail fastener design was also studied. Originally, four rail fasteners were chosen for analysis. These are shown in Figure 7, and are as follows:

(1) English Pandrol rail clip

(2) Swedish fist clip

(3) German Delta clip

(4) Rigid-type clips designed for American MR-3 concrete ties.

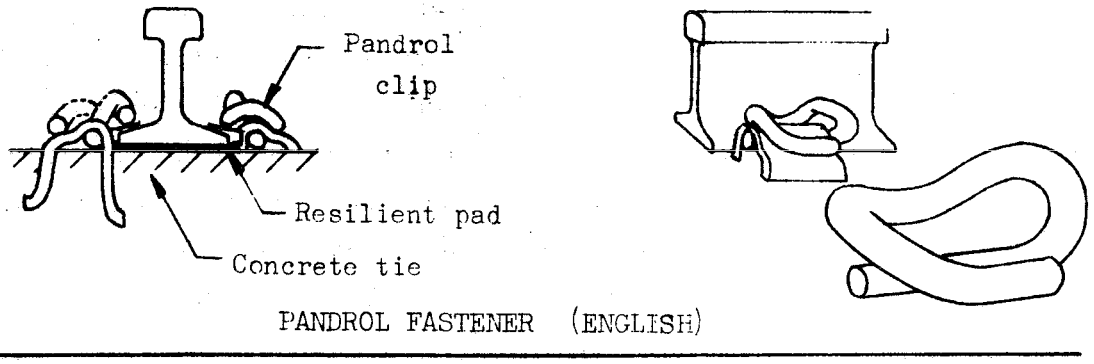

PANDROL FASTENER (ENGLISH)

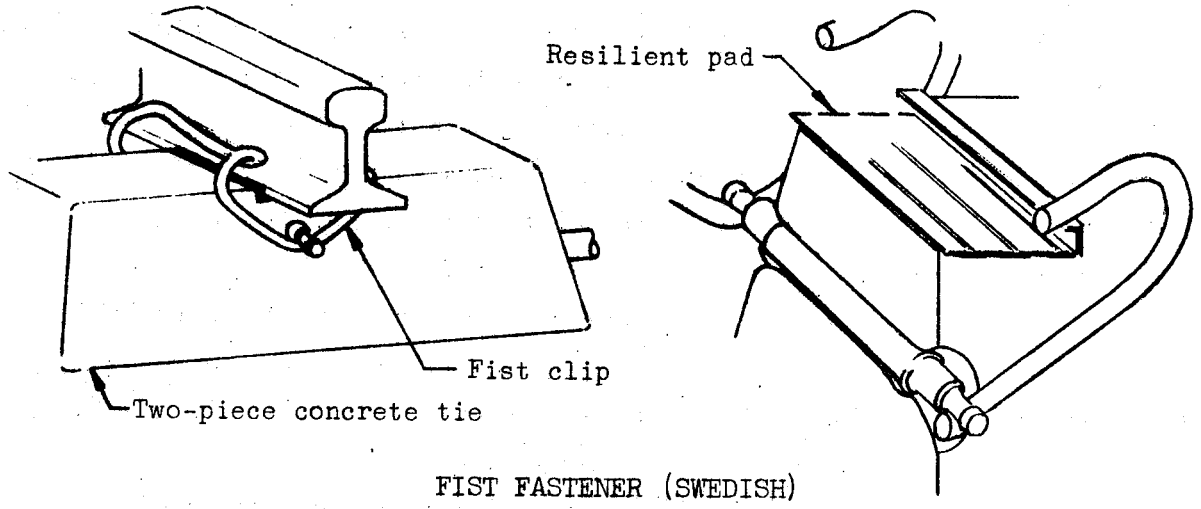

FIST FASTENER (SWEDISH)

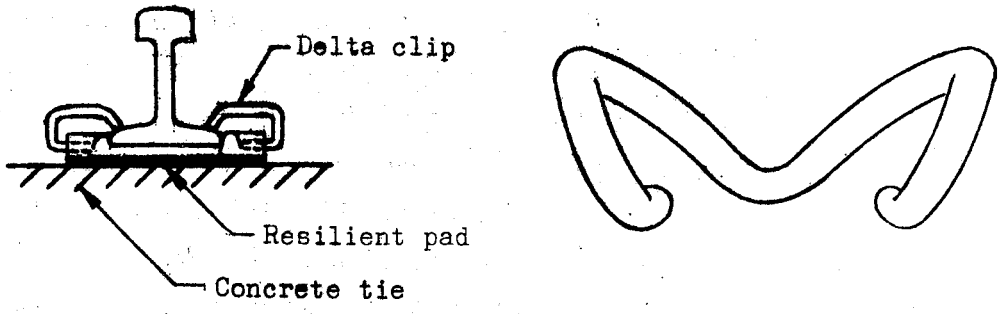

DELTA FASTENER (GERMAN)

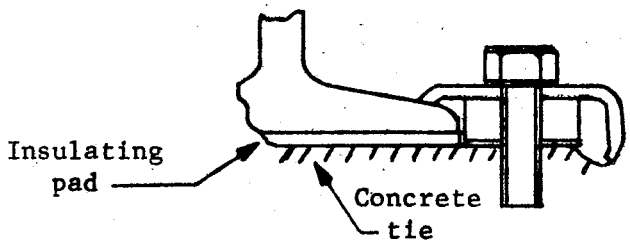

RIGID-TYPE FASTENER FOR AMERICAN MR-3 TIE

FIGURE 7. FOUR TYPES OF RAIL FASTENERS FOR CONCRETE CROSSTIES

However, information for the Swedish and German fasteners required for representing them in a computer program (to determine stresses and deflections as a function of the load) was not received in time to be included in the study, and as a result a more general study of fastener design was made.

The Pandrol clip was, however, represented on the computer, and good correlation of computer results with measured stresses and deflections was obtained, indicating the analysis technique to be a valid one and applicable to other fasteners.

Although there are enough rail fasteners of seemingly different design on the market to make an analysis appear formidable, from a functional standpoint they can all be represented by a relatively simple model. Since their purpose is to resist gross rail movement under loads induced by the environment and by train passage, and in practice they do this by supplying a downward restraining force on the rail, a basic criterion for functional effectiveness is how consistently the hold-down load is applied. The three most important factors which determine this are the initial hold-down force, the spring rate of the rail clip itself, and the spring rate of the resilient pad (if any). If the clip spring rate is low, a more constant clamping force will be maintained than if the spring rate is high; furthermore, the cyclic stress variation will be minimized, a factor contributing to longer life. Life, of course, depends on the ratio of applied stresses to allowable stresses, and no attempt was made to predict the life of any of the fasteners analyzed.

Of the four clips examined, three can be classified as low spring-rate types and the fourth (including several of the same general design) as a high spring-rate type. Table 4 summarizes pertinent characteristics of these four fasteners, and points out the sensitivity of the high spring-rate type clip to dimensional variations. Therefore, while with this clip the initial clamping force is high, dimensional changes due to wear, yielding, or other causes can quickly relieve the preload. The stress levels are such that it would seem that yielding could easily occur.

TABLE 4. RAIL FASTENER CHARACTERISTICS

Type	Pandrol	Swedish Fist	German Delta	American for MR-3 Ties
Recommended installed hold-down force (per rail)	3000 lb (1500 per clip)	4500 lb	--	10,000 lb (5,000 per clip)
Estimated spring rate of clip, installed	5000 lb/in.	6000 lb/in.	8500 lb/in.	> 70,000 lb/in.
Estimated clip stress at (maximum) hold-down force, listed above	156,000 psi	--	--	361,000 psi*
Estimated stress variation in clip due to 22,500-lb wheel load	5510 psi	--	--	43,400 psi
Change of hold-down force due to dimensional variation of 1/16 inch (due to wear, tolerances, yielding, etc.)	312 lb	375 lb	530 lb	4370 lb
Approximate loss of clip hold-down force during wheel passage	53 lb	100 lb	150 lb	600 lb

* This high stress level cannot exist. Either the clip yields, or it is considerably stiffer, meaning a higher spring rate but lower stress.

The numbers shown in the table were based on a rail pad stiffness of 700,000 pound/inch. Lower pad stiffnesses (which are desirable to minimize impact effects on the tie-supported structures) increase the clamping force loss for a given clip stiffness; however, with the low-rate clips this loss is still small (see text).

While data on the Delta clip was not available, similarities indicate stresses to be comparable to those in the Swedish fist clip.

In addition to fastener resistance to applied vertical loads, their performance under lateral load and their electrical insulation properties were considered briefly. These two properties are sometimes interrelated; for example, the clips for MR-3 ties provide positive lateral restraint to the rail base in the form of a shoulder on the steel clips. Insulation would be obtained only if the clip-to-tie bolt or tie bolt-to-tie connection were insulated. On the Swedish clip, the longitudinal pins through the tie beneath each rail is insulated from the tie, while in the Pandrol clip a small insulating pad is used between the clip and rail at the hold-down location.

While there are many other factors which must be considered in fastener design--for example, bolt stresses, elongation, stress and chemical corrosion, etc.--they were not considered in this analysis of basic load-deflection-stress relationships.

CONCLUSIONS

The results of the static and dynamic analyses showed that in general (within the limits mentioned later) a soft rail spring rate at the rail is desirable to minimize wheel-rail dynamic forces caused by wheel and rail profile irregularities, while a stiff support structure is desirable to minimize the pressures and deflections transmitted to the ballast and subgrade.

While these are conflicting requirements, they can be met by the use of resilient pads between rail and support--whether the support is provided by ties or longitudinal beams. The proper resilience of the pads is a function

of the stiffness of the other components, which will vary from one installation to another. However, computer studies such as those described in this report enable the proper resilient pad stiffness to be obtained as a function of these other factors, including rail size, rail fastener stiffness, tie spacing and bearing area, and ballast and subgrade properties.

To obtain the required stiff support structure which will minimize ballast and subgrade pressure, increased effective bearing area per unit length along the track is required. For tie structures, this is accomplished by increasing tie bearing area or decreasing tie spacing, or both. The advantage of, say, a concrete tie with increased bearing area, can be lost by excessive tie spacing.

Longitudinal slab or beam-type structures have the advantage of distributing load longitudinally, so that even if their actual bearing area per unit length were the same as for a tie structure, the bearing pressures would be lower because of the increased longitudinal stiffness (compared with that of the rail alone) and the greater uniformity of pressure beneath the continuous beam-type structure.

From an examination of the basic functional requirement of rail fasteners--that is, providing a consistent clamping force to the rail--it was concluded that the vertical spring rate of the rail fastener assembly is a most important characteristic, and that this spring rate should be low rather than high. To determine whether any specific fastener will maintain its original clamping force over long time periods with repeated loadings, load-stress-deflection characteristics of all fastener components should be determined; stresses should be low enough to provide the required number of load cycles. For spatially complex three-dimensional rail clips now available commercially, digital computer beam programs can be used for quickly determining load-stress-deflection characteristics.

Only after these basic functional requirements have been met should other fastener criteria such as cost, simplicity, and ease of installation and removal, etc., be examined. The point here is that a cheap fastener which does

not fulfill the basic functional requirements will cost more in the long run, and the first consideration should be an examination of the functional requirements.

To carry on the general program of track structure analysis, a considerable amount of additional work needs to be done. Specifically, the following is suggested:

(1) Conduct a series of field measurements on various railroads to obtain actual track response for correlation with calculated response. Static response (overall spring rates) as well as dynamic response would be obtained, both vertical and lateral.

(2) Using the data obtained above, refine and validate the computer model of the track structure and investigate track structure response further.

(3) Consolidate information obtained above into the form of design data which could be used for the design of high-speed track structures.

TECHNICAL WORK

The technical work was divided into two categories--analysis of particular track structures, and the analysis of four rail fasteners.

Analysis of Track Structures

The eight track structures which were analyzed are listed below, and were illustrated in Figures 1-6.

(1) Conventional track structure (rail-wood ties-ballast, as shown in Figure 1)

(2) Conventional track structure with resilient pads between rail and wood ties

(3) Conventional track structure (rail-concrete ties-ballast, as shown in Figure 2)

(4) Conventional track structure with resilient pads between rail and concrete ties

(5) Conventional rail supported by bearing plates on precast concrete pads connected diagonally by steel tie-bars (Dutch "zig-zag" configuration, as shown in Figure 3)

(6) Conventional rail supported by resilient pads and oak stub ties on a continuous cast-in-place concrete slab (Louis T. Klauder Structure No. 1, shown in Figure 4)

(7) Conventional rail supported by resilient pads on precast longitudinal reinforced concrete beams joined laterally at 10-foot intervals by concrete tie beams and through-bolts (shown in Figure 5)

(8) Conventional rail supported by resilient pads and bearing plates on precast, prestressed concrete beams of 18-foot length, which, in turn, are supported at 18-foot intervals by precast hollow cylindrical concrete piles and lateral precast concrete tie beams (Louis T. Klauder Structure No. 8, shown in Figure 6).

Analysis of these track structures included their representation on analog and digital computer programs, and calculation of stresses, deflections, soil pressures, etc., under applied static and dynamic loads.

Mathematical Representation of Track Structures

In order to represent the five track structures on the analog computer, it was necessary to convert them from actual track structures to distributed parameter systems and finally to lumped-parameter systems in which each track structure was represented by springs, dampers, and masses in series.

The steps involved in this conversion are indicated in Figure 8. For the track structures involving tie-supported track, the support for each tie can be represented as a spring whose spring rate is a function of the ballast and subgrade properties. As the calculation of this ballast-subgrade spring rate is

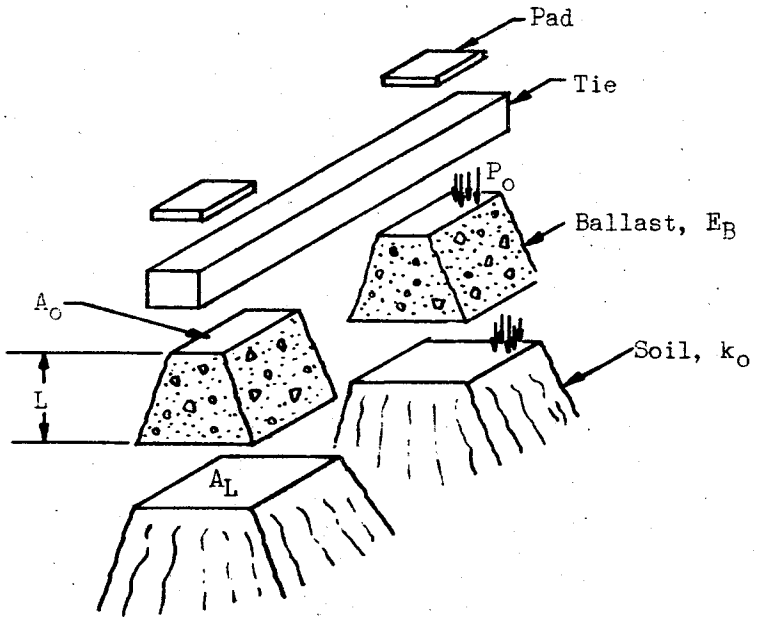

(a) Conventional Track Structure

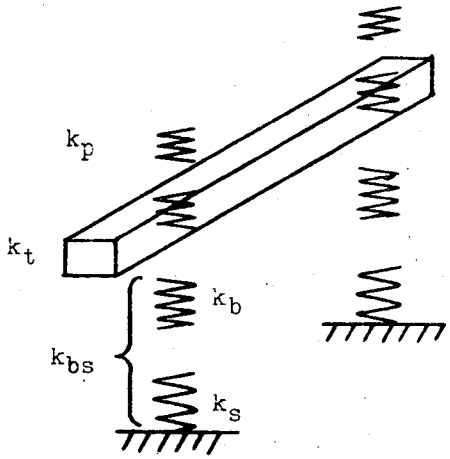

(b) Spring Rates of Track Components

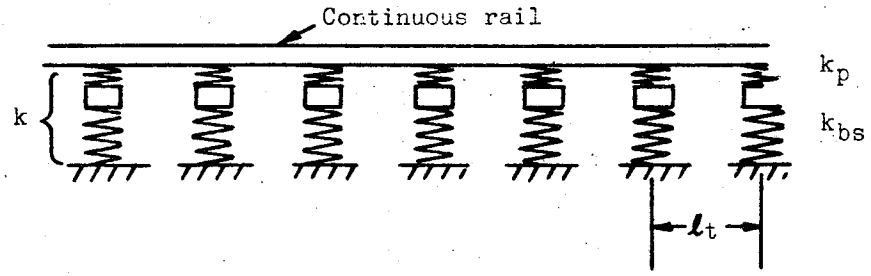

(c) Beam on Continuous Elastic Support

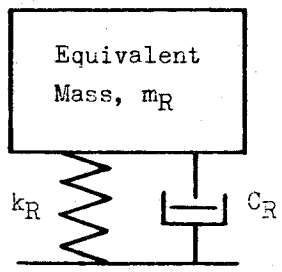

(d) Dynamic Equivalent of Beam on a Continuous Elastic Support

FIGURE 8. PROGRESSIVE STEPS IN THE DEVELOPMENT OF A SUITABLE DYNAMIC MODEL OF A CONVENTIONAL TRACK STRUCTURE

not straightforward, a considerable effort was devoted to the development of a rational method for calculating the overall track stiffness from known properties of the ballast and subgrade. Unfortunately, the area of soil mechanics is one where precise answers usually cannot be obtained, and this case was no exception.

The first step was to examine various methods of calculating the stiffness of the ballast and subgrade when loaded by a rectangular area such as a railroad tie. Three methods were considered:

(1) Boussinesq equations

(2) Elasticity theory for plate loading

(3) Approximate method considering the affected volume of soil to be a pyramid of uniform pressure.

It was concluded that Boussinesq equations are not directly applicable for spring rate calculations because they assume point or line loading and yield infinite deflections under the point of load application. They are mainly useful for calculating stresses or pressures in the vicinity of a localized load.

Elastic theory predicts practically the same spring rates for two ideal cases of area loading: one case gives an average deflection of a uniform pressure-loaded area, and the other gives the uniform deflection under a rigid plate load. The main drawback of these equations is that two layers (ballast and soil) are not easily handled, and calculations based on a single layer yield results which do not agree with actual measured values. Equations accounting for two layers of different homogeneous materials or increasing stiffness with depth are more realistic, but are much too complex to be generally useful.

The pyramid approximation assumes uniform (but different) pressure at every depth to infinity and uniform deflection of the loaded area, and neglects the material outside the pyramid. The equation for stiffness is the same form as that given by the theory of elasticity, but is simpler and can account for two or more layers of different materials. The stiffness of the pyramid is highly dependent on the angle of its sides (the "angle of internal friction" of the soil), which determines the rate at which the load is assumed to spread out as it is transmitted downward (see Figure 8-A). With a particular choice of this angle, the stiffness is the same as that predicted from the theory of elasticity; if a steeper angle is chosen, the stiffness will be less.

It was concluded that the pyramid method was the most applicable one. Figure 9 is a plot of the stiffnesses of the soil and ballast calculated by the pyramid method, for a given bearing area 9" x 25.5", corresponding to a tie with half its area acting in bearing. (The spring rate is a function of the shape of the bearing area, as well as its size.) The depth of the ballast was assumed to be 2 feet, and the angle of internal friction was assumed to be 20 degrees. Using values of k_b and k_s from this figure, the overall spring rate of the ballast and soil in series can be calculated from the expression

$$k_{bs} = \frac{k_b \, k_s}{k_b + k_s} \quad . \tag{1}$$

The most uncertain factor involved in the determination of the overall spring rate is the so-called subgrade modulus of the soil beneath the ballast (k_o). It is affected by the size and shape of the area loaded, the moisture content and the degree of compaction of the soil, as well as the basic material, and so is not truly a material property. In general, however, it varies between 100 and 500 psi/in. for undisturbed earth, and for prepared subgrades such as those beneath new highways and railroads an average value is probably 150 psi/in.--with 200 psi/in. being on the high side. Values of ballast E_b are generally on the order of 20,000 to 40,000 psi.

Values of ballast-soil stiffness obtained from the equation above can then be used in the representation of the track structure as a continuous beam supported on a continuous elastic foundation (Figure 8-C). Straightforward methods are then used to convert this distributed parameter system into a lumped-parameter system necessary for the analog computer representation (Figure 8-D).

Considering the load on one rail, the spring rate of the half tie, tie plate, resilient pad, ballast, and soil in series is approximately

$$k = \frac{k_{bs} \, k_p}{k_{bs} + 2k_p} \quad . \tag{2}$$

The factor of 2 is introduced in Equation (2) to account for the continuity of the ballast and soil deflection between adjacent loaded ties. This continuity is neglected in the elastic foundation model and experiments indicate

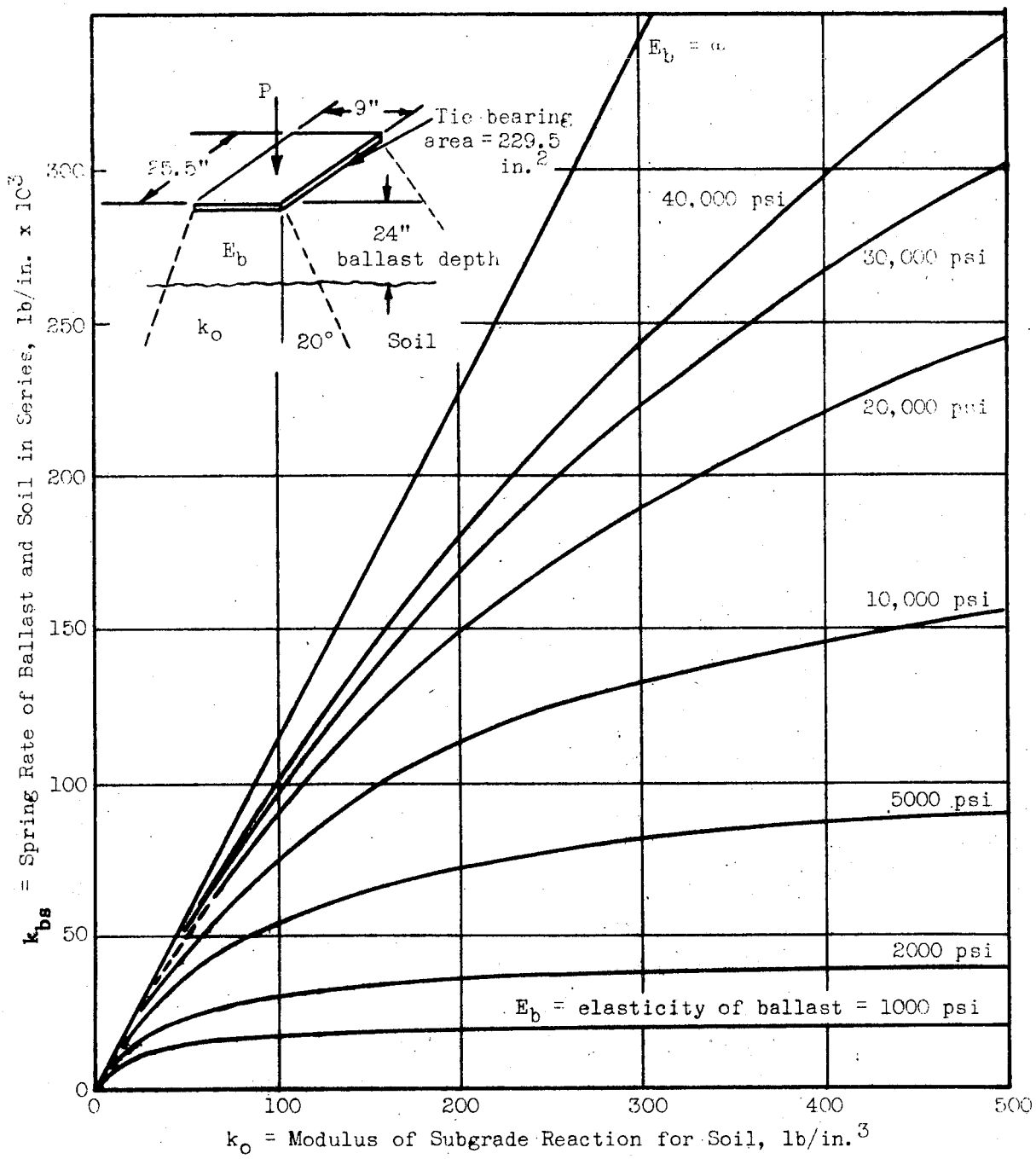

FIGURE 9. OVERALL VERTICAL SPRING RATE OF BALLAST AND SUBGRADE

that each of the ties supporting a loaded rail is approximately twice as flexible as when it is loaded alone.

Knowing k_{bs}, the overall spring rate (k_R) of a rail supported on a row of these springs (Figure 8-A) can be calculated. For example, Figure 10 shows overall spring rates for three different rails and four different tie spacings.

The track structures having continuous longitudinal-beam type support are not amenable to this type of model; for them a digital computer program for general structures was used. In this computer program, structures were represented by a series of beams connected together at rigid node points. Deflections of the node points, together with axial forces, shear forces, bending moments, and stresses in the beams, are calculated for any type of loading condition. Both bending deflection and shear deflection of the beams are taken into account.

Figure 11 shows the longitudinal twin-beam track structure and the model used to represent it on the computer. A total of 97 node points and 129 beams were used in order to obtain an adequate representation (more than two 39-foot beams and three joints) of the track, including the resilient fasteners and the resilient soil beneath the structure. Each fastener was represented by a vertical beam sized to give a vertical spring rate of 750,000 lb/in. each and spaced at 30-inch intervals to give a resilience of 25,000 lb/in. per inch of length along the rail. This value was determined earlier from the analog computer analysis to be an optimum value for a relatively stiff longitudinal-beam type structure, based on wheel-rail dynamic forces resulting from track profile irregularities. The bending rigidity of the vertical beams representing the fasteners was deliberately made small to allow complete angular and longitudinal freedom between the rail and the concrete support beam. It was determined by hand calculation that the vertical beams used to represent the soil could be placed at intervals of 60 inches without significantly affecting the accuracy. These beams were then sized to represent two different soils. The two soils were assumed to have bulk moduli of 100 psi/in. and 500 psi/in. respectively, and these values in conjunction with the 24-inch wide beam gave foundation stiffnesses of 2400 and 12,000 lb/in. per inch of length along the beam respectively. A 132-pound rail was used, and a concrete beam having an

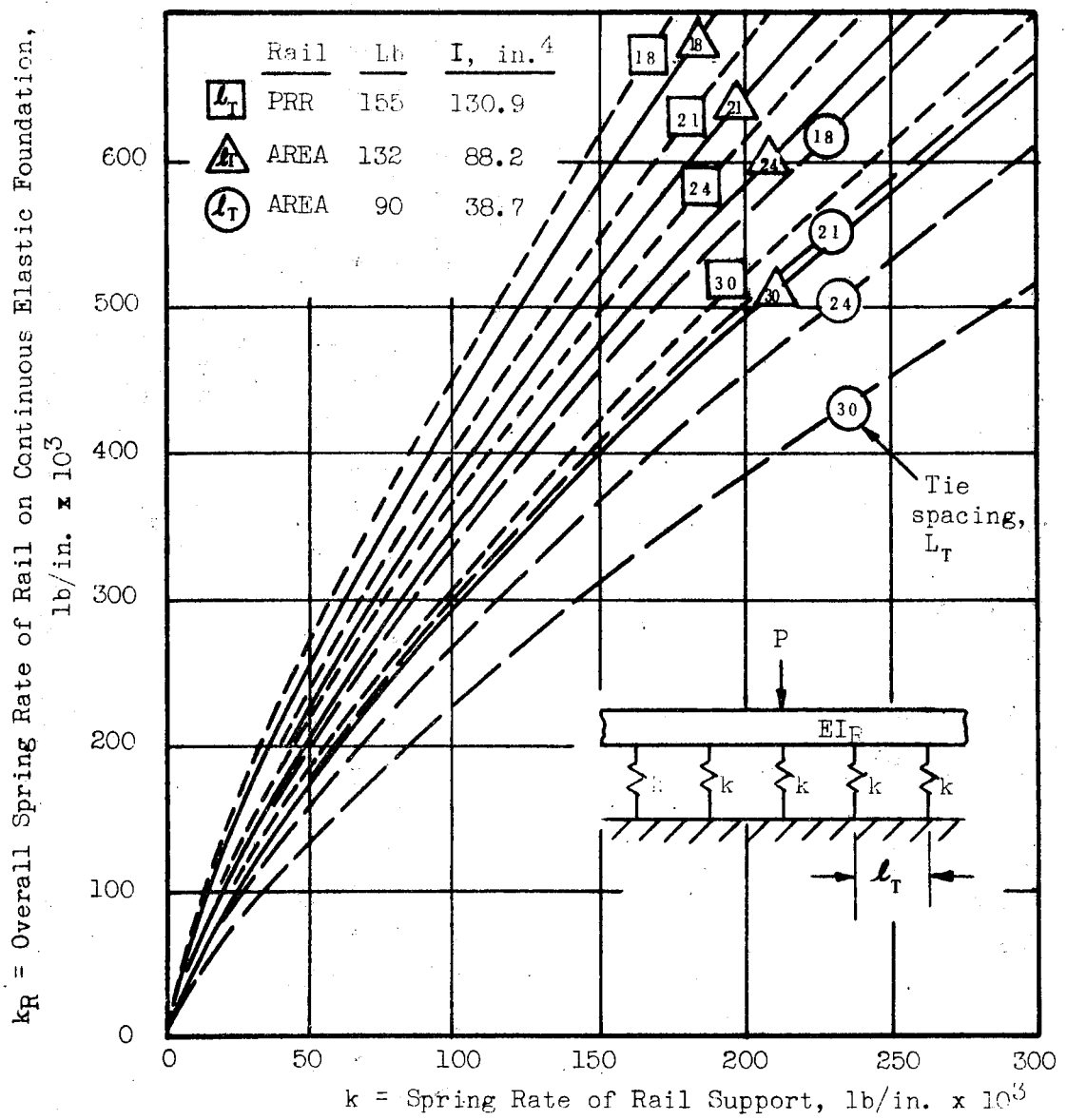

FIGURE 10. TRACK STRUCTURE SPRING RATE AS A FUNCTION OF RAIL, TIE, AND SUBGRADE CHARACTERISTICS

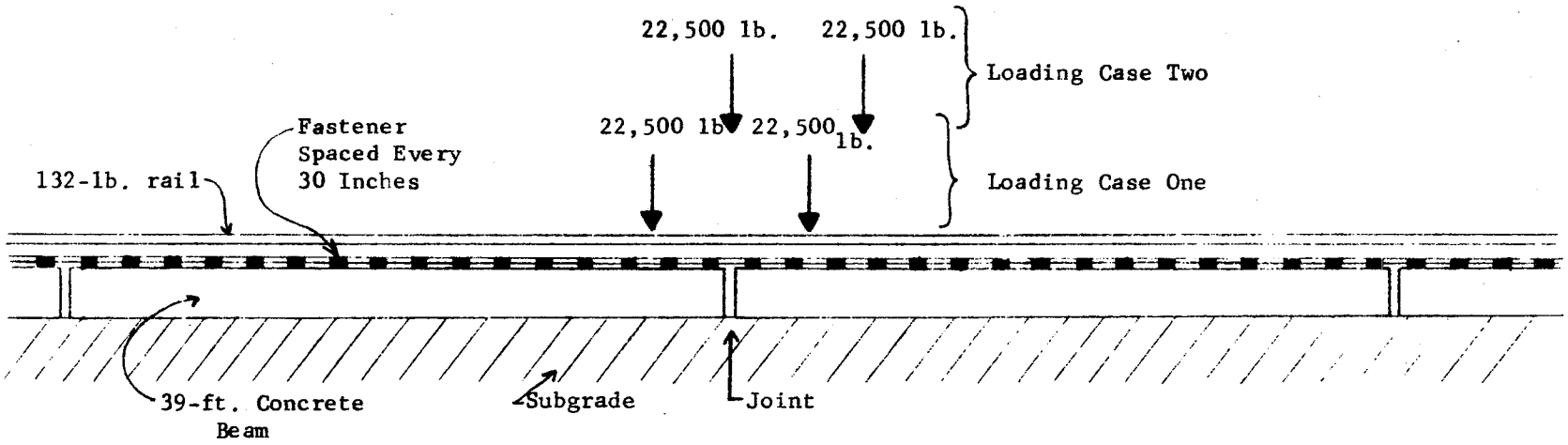

(a) Longitudinal Beam Track Structure

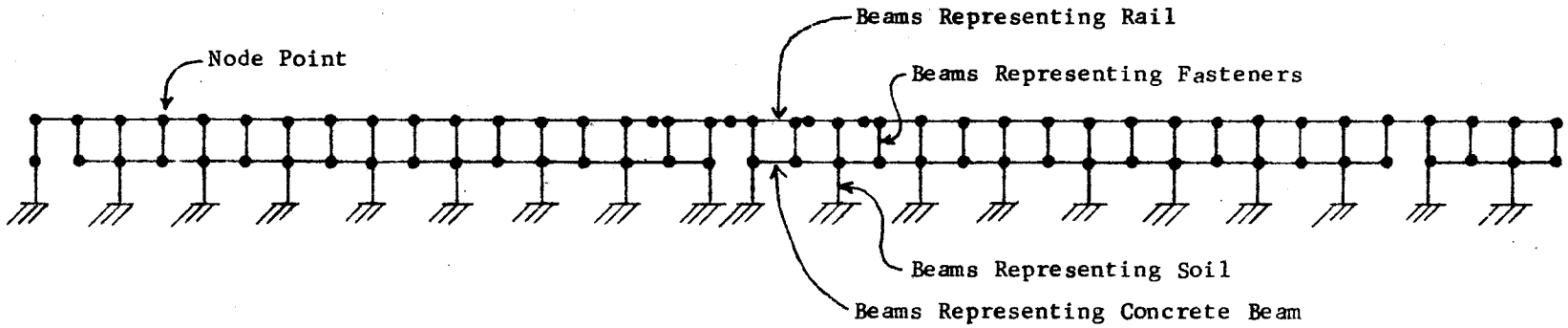

(b) Digital Computer Model of Track Structure

FIGURE 11. REPRESENTATION OF TWIN LONGITUDINAL BEAM STRUCTURE ON DIGITAL COMPUTER

area of 305 $in.^2$ and an area moment of inertia of 6860 $in.^4$ was used (JPI Drawing No. JP67-48-A, dated August 14, 1967, and August 29, 1967).

Response to Static Wheel Loads

To determine such factors as overall spring rate, rail stress, ballast pressure under ties, etc., the response of the various track structures to a wheel load of 22,500 pounds (assuming one axle is loaded to 45,000 pounds) was calculated. Values which were calculated for the tie-supported track structures are shown in Table 5, and were summarized previously in Table 1.

Some observations can be made from this table. First, it is seen that the concrete tie track with resilient pads has a greater overall stiffness than the wooden tie track without pads, when the tie spacing is the same. The reason for this is not that the concrete ties themselves are very much stiffer than wooden ones, but that they have a larger bearing area, which results in a higher ballast-soil spring rate. Actually, considering only the ties themselves, a concrete tie with a typical resilient pad is much softer than a bare wooden tie. However, when the ties are placed on the same ballast and soil, the overall spring rate of the concrete-tie structure is higher due to its higher bearing area. The larger bearing area of the concrete tie results, of course, in lower ballast and soil pressures. Rail bending stresses are also lower due to the higher stiffness (and lower rail deflections). Note that this discussion assumes the spacing of wood or concrete ties is the same.

When the tie spacing is increased from 21 inches to 30 inches, the overall stiffness drops because there are fewer springs under the rail; the ballast and soil pressures increase because less total area must carry the same load. The rail stress increases because the rail has to span a greater distance, and therefore, bends more under the same load.

A comparison of the conventional track structures with the Dutch "zig-zag" track design shows that the latter's combination of low bearing area and widely spaced tie blocks results in a system with the highest soil and

TABLE 5. SUMMARY OF PARAMETERS DEFINING TIE-TYPE TRACK STRUCTURES (WHEEL LOAD = 22,500 POUNDS)*

Structure Number	1		2		3-a		4-a		3-b		4-b		5	
Structure Description	Std. 9" x 7" x 102" Oak Ties				MR-3 Concrete Ties				MR-3 Concrete Ties				Dutch Zig-Zag	
	Without Pad		With Pad		Without Pad		With Pad		Without Pad		With Pad		Without Pad	
A_o (in.^{2})	229.5				396				396				240	
A_L (in.^{2})	1140				1490				1490				1106	
m_t (#sec^2/in.^{2})	0.0225				0.0333				0.0333				0.0357	
m_r/m_t	0.425				0.288				0.288				0.267	
ℓ_t (in.)	21				21				30				30	
k_o (#/in.^{3})	100	500	100	500	100	500	100	500	100	500	100	500	100	500
k_{bs} (10^3 #/in.)	98	330	98	330	132	450	132	450	132	450	132	450	96	319
k_p (10^3 #/in.)	∞		700		∞		700		∞		700		∞	
k (10^3 #/in.)	49.0	165	45.8	134	66.0	225	60.3	157	66.0	225	60.3	157	48.2	160
k_R (10^3 #/in.)	228	562	215	480	280	700	263	540	212	535	200	415	168	422
m_R (#sec^2/in.)	2.20	1.61	2.22	1.69	2.97	2.18	3.05	2.41	3.21	2.38	3.32	2.64	3.73	2.83
$f = \frac{1}{2\pi}\sqrt{k_R/m_R}$ (cps)	51.2	94.1	49.5	84.8	48.9	90.2	46.8	75.3	40.9	75.4	39.0	63.0	33.7	61.4
y_o (in.)	0.099	0.040	0.105	0.047	0.080	0.032	0.086	0.042	0.106	0.042	0.113	0.054	0.134	0.053
p_o (psi) ballast	21.1	28.8	20.8	27.4	13.4	18.2	13.0	16.6	17.6	24.0	17.2	21.4	27.0	35.4
p_L (psi) subgrade	4.2	5.8	4.2	5.4	3.6	4.8	3.5	4.4	4.7	6.4	4.6	5.7	5.9	7.7
σ_{rail} (10^3 psi)	10.0	6.6	10.0	6.8	8.5	6.3	9.3	7.3	9.8	6.6	10.1	8.0	10.6	8.1

* Rail Size: AREA 132 lb; Ballast Modulus, 35,000 psi; Ballast Depth, 24 inches.

ballast pressures, the highest rail stress, and the lowest spring rate, even though no resilient pad is used. Because of the high pressures and stresses, this structure appears to be inferior to conventional track from the standpoint of long-term stability.

For the beam-type track structures having continuous support from the soil, two loading cases were investigated, as shown in Figure 11-A. In each case, the loads imposed by one four-wheel truck (two loaded axles) were used. The first case considered the truck axles straddling the joint, and the second considered one axle of the truck directly over the joint. It is believed that these two cases bracket the range of variables. Wheel loads were 22,500 pounds.

The four deflection curves resulting from the two soils and the two loading cases are shown in Figures 12-A and 12-B. The deflection of the concrete beam is the same as the deflection of the supporting soil beneath the beam, and is, therefore, proportional to the bearing pressure exerted on the soil. The difference between the rail and beam deflection represents the deflection of the resilient rail fasteners.

The stiffness of the overall track structure is only slightly lower at the joint, as indicated by the maximum deflection of the rail when a wheel load is applied directly above the joint. Further shown in the curves is that wheel loads near one joint in the beam do not significantly affect the deflections or pressures at the adjacent joints.

Figure 12-C shows the deflection curve for an identical but continuous track structure for the same wheel loading used on the noncontinuous structure. Only one soil modulus was considered for this continuous structure, namely, 100 lb/in^3., and the two separate loading cases discussed above result in identical deflection curves for the continuous structure; therefore, only one case is shown in the figure. Comparing this curve with that of the noncontinuous structure in Figures 12-A and 12-B shows the effects of a joint in the longitudinal beam.

The point which is brought out by the curves is that for the static case and for the values of soil and pad stiffness considered here, the rail does a fairly adequate job of bridging the joint in the beam. This is evidenced by

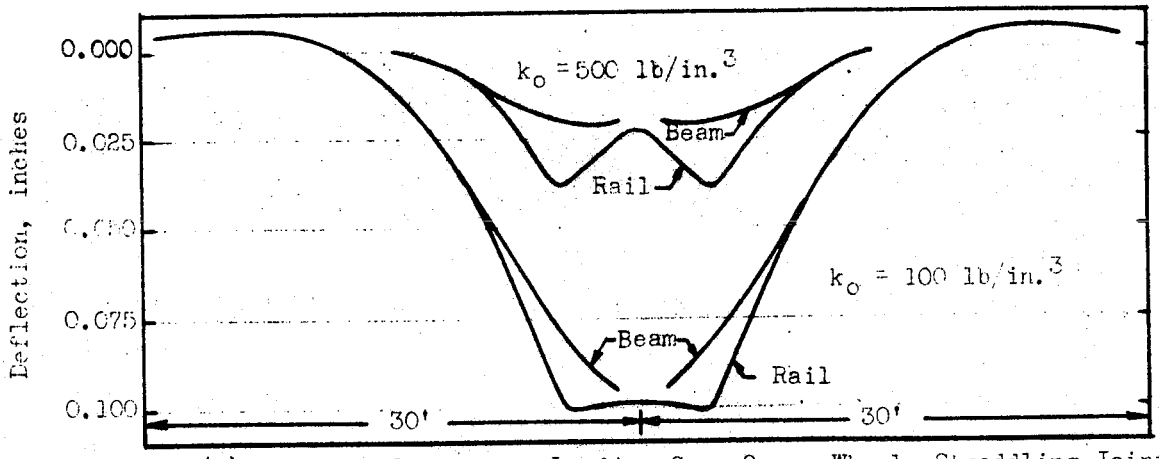

(a) Jointed Structure; Loading Case One - Wheels Straddling Joint

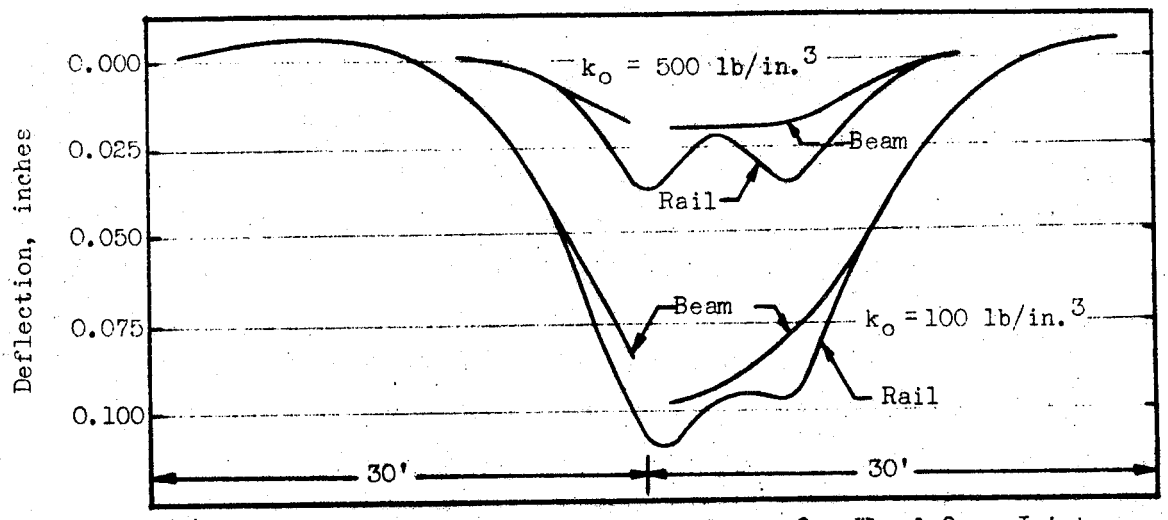

(b) Jointed Structure; Loading Case Two - One Wheel Over Joint

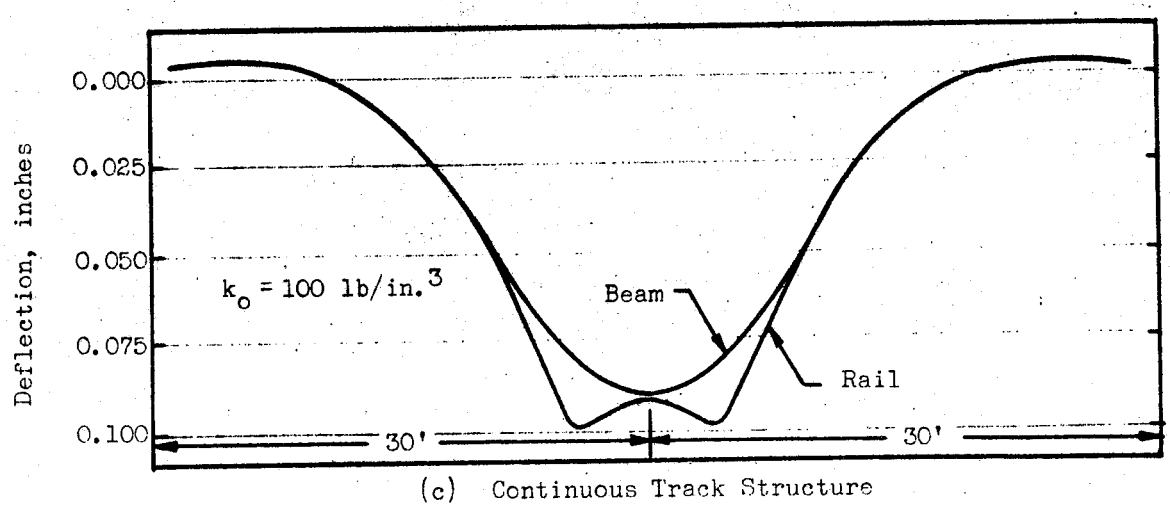

(c) Continuous Track Structure

FIGURE 12. RAIL AND BEAM DEFLECTION FOR LONGITUDINAL BEAM TRACK STRUCTURES WITH AND WITHOUT JOINTS (I_{RAIL} = 88.6 in.^{4}, I_{BEAM} = 6860 in.^{4}, K_{PADS} = 25,000 lb/in.^{2}, WHEEL LOAD = 22,500 lb)

the fact that the deflection of the beam with the joint is only slightly greater than the deflection of the continuous beam (about 11% greater). There will, of course, be a "soil stress-concentration factor" at the joints, particularly for the case shown in Figure 12-B where a considerable amount of vertical shear is present at the soil in the vicinity of the joint.

In addition to the deflections of the rail and concrete beam, the computer program calculates the stresses in these components. The important peak stresses for the three different structures and soil combinations are included in Table 2. The peak bending stress in the rail for the two noncontinuous structures occurs when one axle is directly over the joint (loading case two in Figure 11-A). On the other hand, the peak bending stress in the concrete beam occurs when the axles straddle the joint (loading case one in Figure 11-A). Assuming a 1000-psi precompression in the concrete, the total peak compressive stresses are 1282 psi and 1330 psi for the beams.

The Louis T. Klauder structure No. 8 was analyzed on the computer in a similar manner. The beam model used to represent the structure consisted of 124 beams and 92 node points, and represented approximately 72 feet of track, including 4 complete 18-foot beams and 5 pile foundations. From the available information, the concrete beams were estimated to have an area of 2110 in^2. and an area moment of inertia of 750,000 in^4. A 132-pound rail was again used. The stiffness of the individual pads was increased slightly, because of the larger spacing, in order to maintain the resilience of 25,000 lb/in. per inch of length along the rail. The vertical stiffness of piles is dependent on many factors and is difficult to calculate accurately. The fact that there was no detailed design of the pile foundation made the choice of the vertical stiffness of the piles even more arbitrary. A specific stiffness was not calculated, but from data in soil mechanics texts stiffnesses of 7×10^4 lb/in. and 42×10^4 lb/in. per pile were chosen to cover a reasonable range. The lower value is quite low; however, due to economic considerations and the vast number of piles needed it is expected that eventually a pile of this low stiffness might be encountered. The upper value may be considered more as a typical stiffness.

The same two axle loading cases were considered for this structure as for the beams supported on the ground, and the four resulting deflection curves are shown in Figure 13. Because of the high bending stiffness of the beams they remain essentially straight compared to the overall deflection, and the rail is subjected to considerable bending at the joints in the beam. Quite large deflections (about 0.5 inch) occur under the wheels for a pile stiffness of 7×10^4 lb/in. The peak stresses calculated are shown in Table 2. All of these peak stresses occur for the loading condition where one axle is directly over a joint in the concrete beam.

Finally, the Louis T. Klauder structure No. 1 was analyzed, and data for this structure is shown in Table 2. This structure is almost identical to the Battelle slab-type structure discussed in the Phase I report. Note that it is by far the stiffest structure, and has the lowest bearing pressures and rail and beam stresses.

Response to Dynamic Wheel Loads

The dynamics of several track structures were investigated on an analog computer. Track structures modeled on the analog computer included wooden-tie-track with and without rail pads; MR-3 concrete-tie-track with and without rail pads (ties on 21-inch centers); and the Dutch "zig-zag" track design. The lumped parameters defining these structures are shown in Table 6. Two types of dynamic analysis were made: steady state frequency response to a sinusoidal rail profile input, and transient response to a sudden 1/4-inch step-down in rail profile. For the steady-state analysis, the total system consisted of that portion (one-half) of a 50-ton Budd rapid-transit railcar body supported by one truck, the truck itself, and that length of a continuous track structure associated with the support of one truck, as shown in Figure 14. The vertical deflection response of the wheel-rail contact point was recorded along with the input rail profile, the wheel-rail force, the car-body acceleration, and the deflections of the car body, axle, and bolster, all taken in the vertical direction.

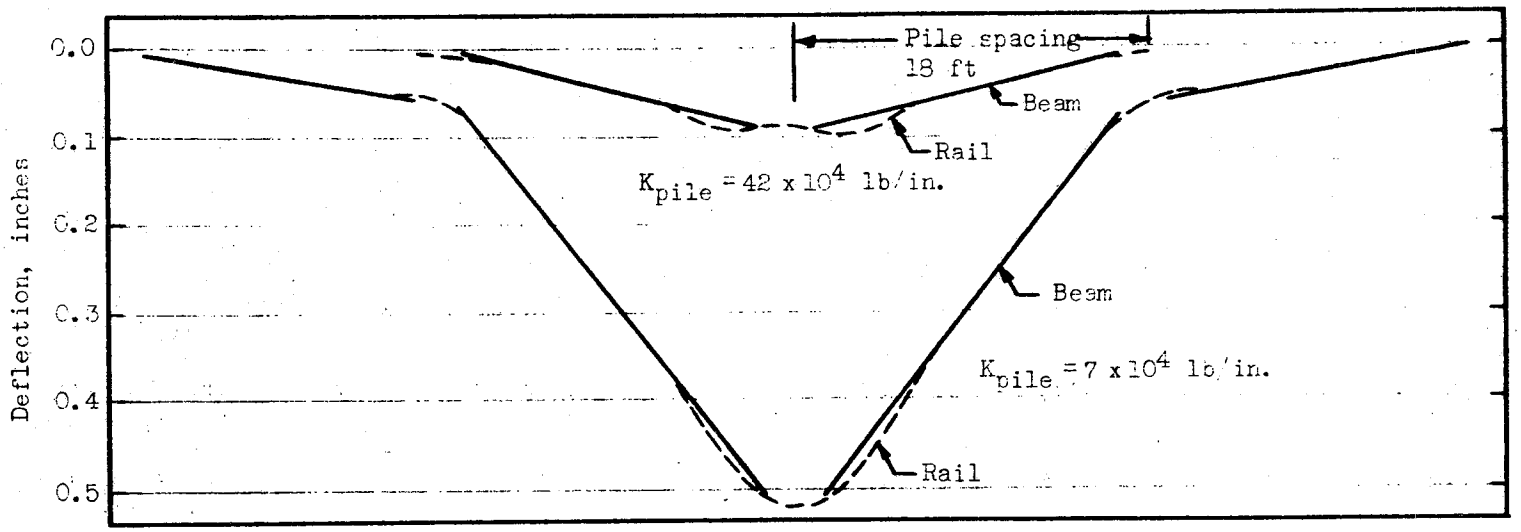

(a) Loading Case One - Wheels Straddling Joint

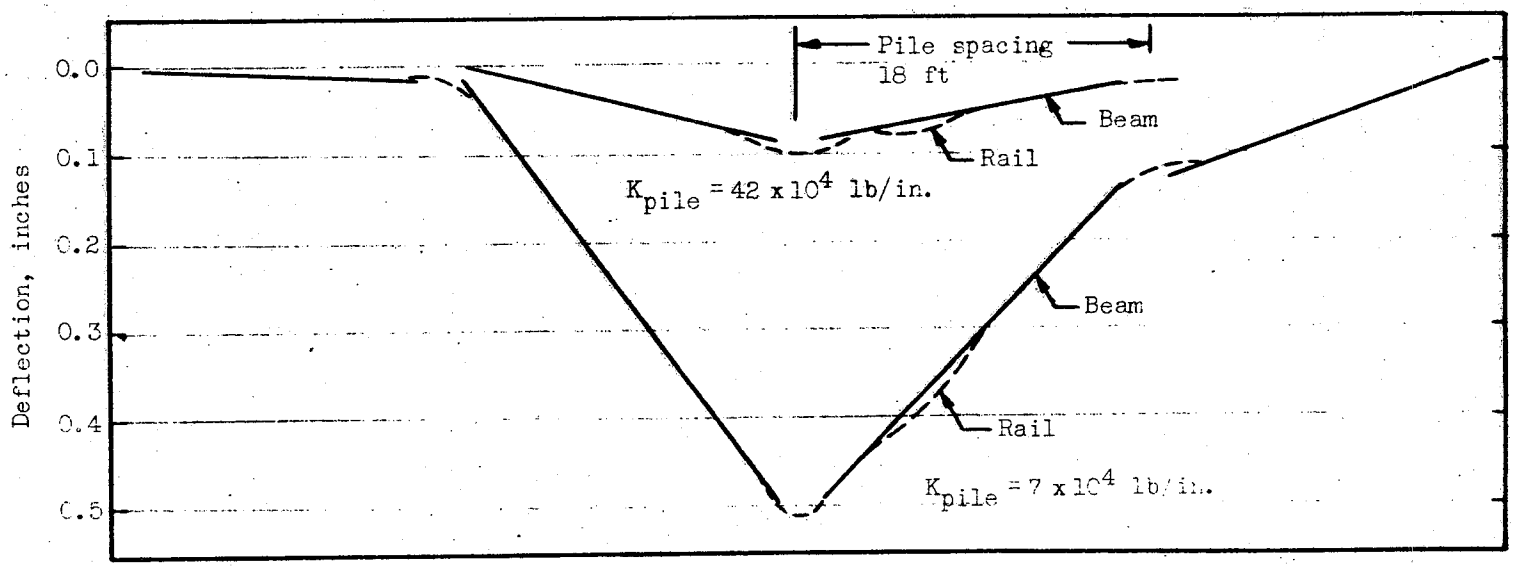

(b) Loading Case Two - One Wheel Over Joint

FIGURE 13. RAIL AND BEAM DEFLECTIONS FOR LOUIS T. KLAUDER STRUCTURE NUMBER 8 (I_{BEAM} = 750,000 IN.^{4}, K_{PAD} = 25,000 LB/IN.^{2})

TABLE 6. SUMMARY OF LUMPED PARAMETERS DEFINING TIE-SUPPORTED TRACK STRUCTURES

Rail Load, P_4 = 22,500 pounds

A.R.E.A. 132-pound rail

Crushed Rock Ballast (E_b = 35,000 psi)

Ballast Depth, L = 24 inches

Weak Soil (k_o = 100 psi/in.)

Structure Parameter (See Figure 7)	21-Inch Tie Spacing				30-Inch Tie Spacing		
	Standard Wooden Ties		MR-3 Concrete Ties		MR-3 Concrete Ties		Dutch Zig-Zag
	Without Pad	With Pad*	Without Pad	With Pad*	Without Pad	With Pad*	Without Pad
Track Structure Overall Spring Rate, k_R (10^3 lb/in.)	228	215	280	263	212	200	168
Equivalent Lumped Mass, m_R (lb-sec^2/in.)	2.20	2.22	2.97	3.05	3.21	3.32	3.73
Natural Frequency of Lumped System, f (cps)	51.2	49.5	48.9	46.8	40.9	39.0	33.7
Average Ballast Pressure Beneath Tie, p_o (psi)	21.1	20.8	13.4	13.0	17.6	17.2	27.0
Average Subgrade Pressure Beneath Ballast, p_L (psi)	4.2	4.2	3.6	3.5	4.7	4.6	5.9
Peak Rail Bending Stress σ_{rail} (psi)	10,000	10,000	8,500	9,300	9,800	10,100	10,600

* Individual pad stiffness = 700,000 lb/in. vertically.

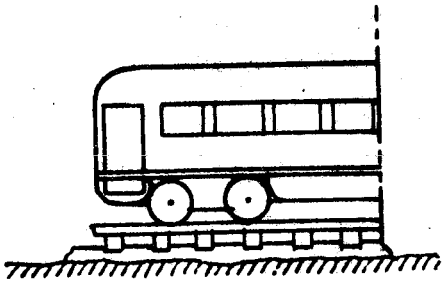

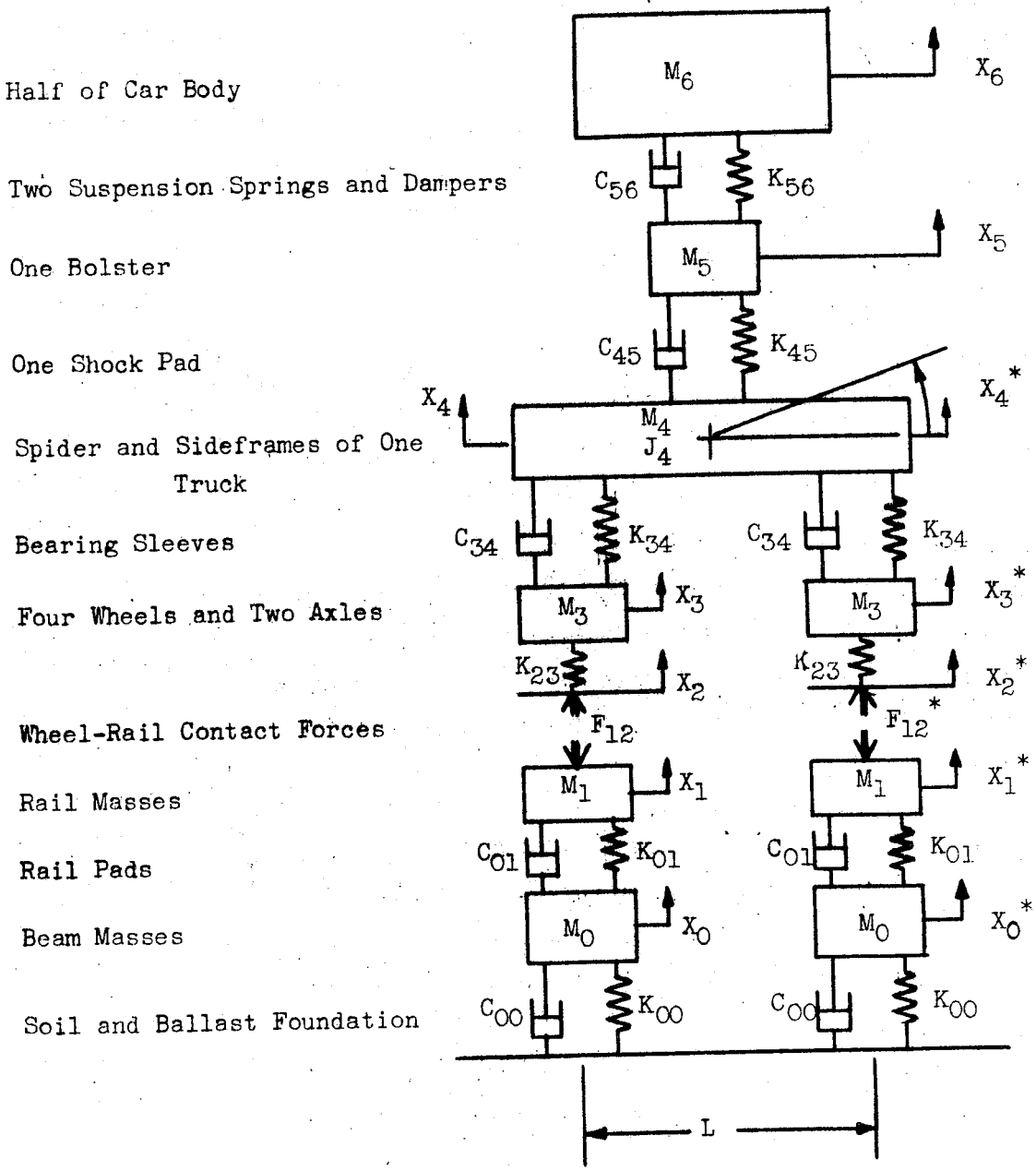

FIGURE 14. ANALOG COMPUTER MODEL USED TO REPRESENT PORTION OF BUDD RAILCAR AND ROADBED

In the transient analysis, the deflection of a fixed point on the rail in response to passing wheel-rail forces was determined. The system in this case consisted of a model of the track structure alone, and the input consisted of the continuous wheel-rail force multiplied by an influence coefficient function to compensate for the changing distance between the wheel and a point on the track. With this method, full force is applied to the track when the passing wheel is directly over the fixed point of interest, zero force to the track when the wheels are a certain distance away, and a varying fraction of the force during the time the wheel is approaching and then leaving a fixed point on the track. The influence coefficient was obtained from the curves for the static deflection of the continuous rail structures.

Three important parameters in these analyses were considered: (1) the car body acceleration--because it is a measure of ride comfort and safety; (2) the wheel-rail force--a measure of the severe localized stresses at wheel and rail surfaces as well as a measure traction and braking potential; and (3) track structure deflection--because this is a measure of basic track stability (which relates to alignment, deterioration, and failure).

Sinusoidal Frequency Response. The results of the steady state analysis are shown in Figure 15, where peak-to-peak car body acceleration per inch of (peak-to-peak) rail waviness amplitude is plotted versus frequency of input. The dashed lines indicate that the rail waviness amplitude, ϵ, was decreased because the wheels began to lift off the rail. The first conclusion that can be made from this graph is that exchanging concrete ties for wooden ones, or inserting a relatively stiff resilient rail pad, or both, have little effect on the car acceleration resonances resulting from steady-state sinusoidal excitation. However, the Dutch "zig-zag" track with its lower natural frequency, reduced the car body acceleration amplitude by 35 percent.

The second conclusion from the frequency response is that on the Dutch "zig-zag" track the frequency at which wheel lift occurs is almost three times as high as on the other four types of track investigated. Wheel-hop is delayed because the Dutch "zig-zag" track resonance condition (when the wheel forces reach their maximum) occurs at a lower frequency and consequently is a lower

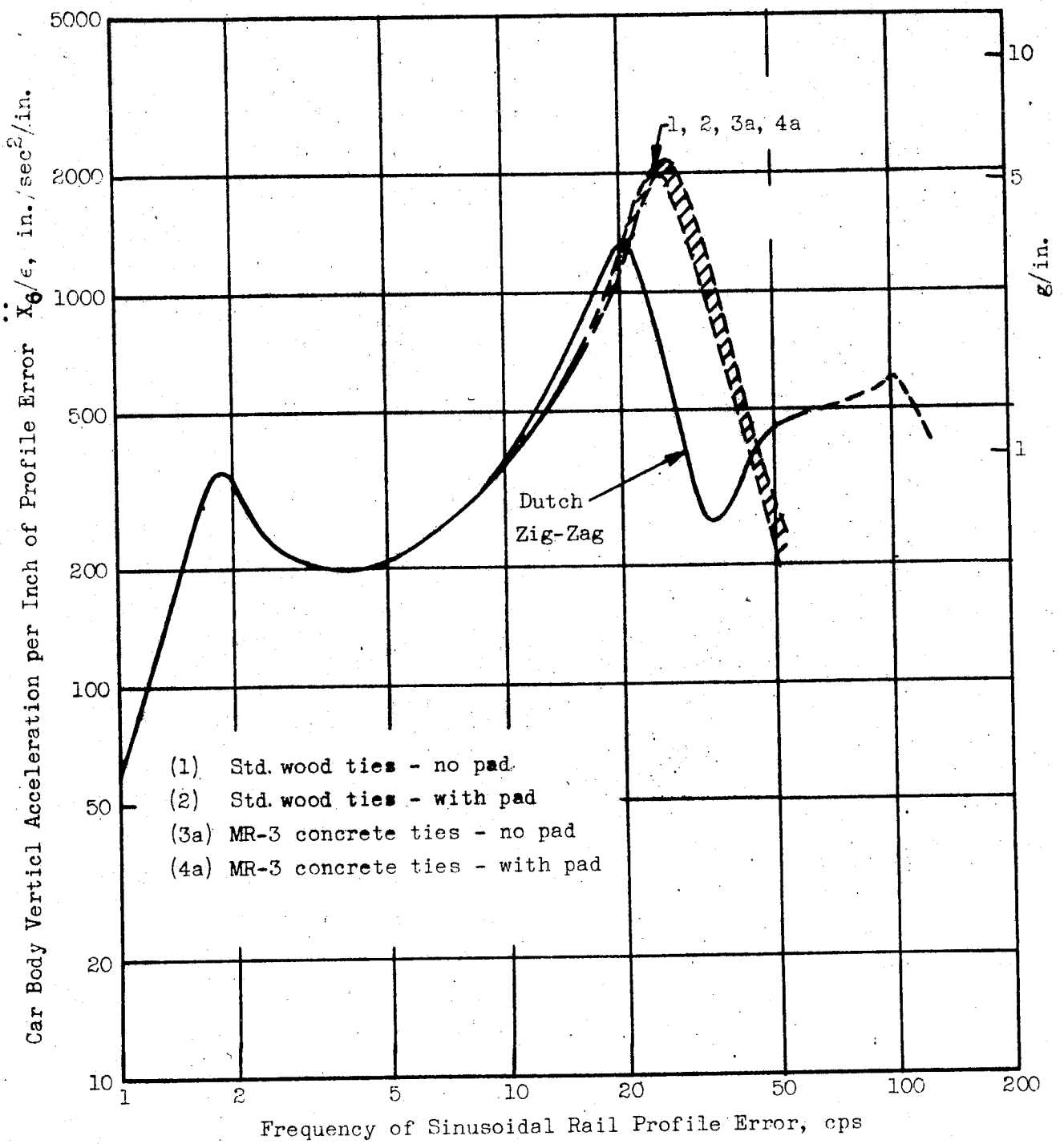

FIGURE 15. CAR BODY VERTICAL ACCELERATION IN RESPONSE TO SINUSOIDAL RAIL PROFILE INPUT FOR VARIOUS TIE-SUPPORTED TRACK STRUCTURES

amplitude oscillation, low enough that the rail acceleration does not exceed one (1) G, meaning that the wheel force due to weight is not relieved. Practically speaking, this means that a softer, more resilient track (such as the Dutch "zig-zag" design) permits a train to maintain a higher speed over a wavy rail profile while maintaining a more constant level of wheel-rail force, resulting in better tractive, braking, and control characteristics. Unfortunately, in the Dutch design, the lower spring rate is obtained by low bearing areas at the expense of high roadbed pressures, rather than by the use of resilient pads.

The displacement of the track structure itself is plotted in Figure 16 as a function of frequency. This can be interpreted as a measure of long term track stability, since the ballast directly under the ties must move an equal amount, and the curve shows the Dutch "zig-zag" ties move slightly more than conventional ties.

Response to Step Inputs. For the mathematical representation of vehicle and roadway commonly used for computer studies, the vehicle is represented by a spring-mass system supported by another spring-mass system representing the roadway, as in Figure 14. The input to the system is usually a displacement representing the vertical profile of the track, highway, or other surface supporting the vehicle.

The wheel-roadway force generated in such a program then represents a force traveling at vehicle speed and located at the wheel. For studies of vehicle response, this is a perfectly proper system, giving as it does the continuous force exciting the vehicle.

For a study of the roadway, however, it is obvious that this force is a transient value with respect to any fixed point on the roadway. The force directly over any point reaches a maximum only when the wheel is directly over that point. An important point to consider is that actual field measurements of track structure response must be obtained by applying instrumentation at one or more fixed locations along the track. It is desirable to validate any mathematical representation of the track structure used on the computer by comparing with measured data from stationary (with respect to length along track) locations; the response of a fixed point on the track is, therefore, a desirable output from the computer study.

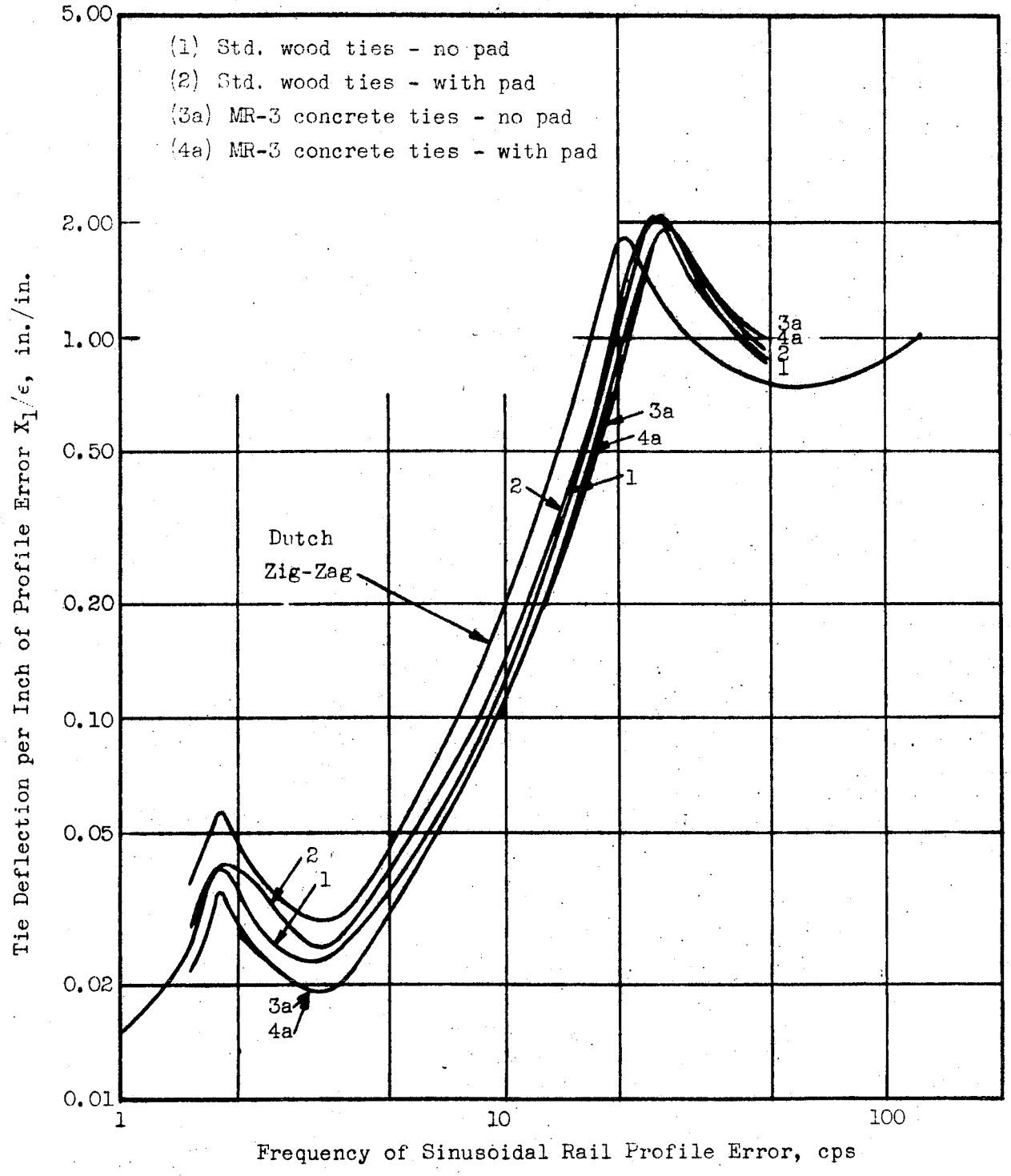

FIGURE 16. TIE DEFLECTION IN RESPONSE TO SINUSOIDAL RAIL PROFILE INPUT FOR VARIOUS TIE-SUPPORTED TRACK STRUCTURE

If the roadway were perfectly smooth and free from profile errors and inconsistencies in the subgrade, etc., measurements show that the curve of deflection versus length for static wheel loads would be approximately the same as the curve of deflection versus time taken at any point on the track structure for conventional train speeds.[1] In the first case, a given distance on the abscissa would represent the longitudinal distance between two wheels on the vehicle, while in the second case this distance would represent the time it takes for the vehicle to travel a distance equal to that between the two wheels. There is, of course, some difference between the static and dynamic vertical deflection due to the inertia and damping effects associated with speed (that is, the rate at which the track is displaced vertically by a passing train), but this difference is negligible up to speeds at which the frequency of wheel load application approaches the natural frequency of the track structure. For a truck with an 8-foot wheelbase and a track structure with a natural frequency of 50 cps, this speed would be 273 mph. Therefore, for practical purposes, the static deflection curve can be assumed to represent the dynamic deflection versus time curve for the case where the rails are perfectly straight, the wheels perfectly smooth, and the track structure has perfectly uniform properties along its length.

However, since this case is not one encountered in practice, the question of practical interest is how to generate the deflection versus time trace of a track having realistic profile errors and nonuniform properties longitudinally.

This can be done by considering the problem as a two-step problem. The first step is to generate the moving wheel-rail force using the conventional representation of vehicle and track, including track profile errors as well as factors such as reduced stiffness at joints, etc. The traveling wheel force generated from this program then can be used as the input to a representation of the track structure itself, using an influence coefficient function to modify the effect of this force on a given point on the rail, according to the distance of this force away from the rail. Obviously, the coefficient is <u>one</u> when the (wheel) force is directly over the fixed point, and drops to zero at some distance away from the point, this value depending on the track structure design.

This procedure was used for the transient analysis of the track structures, except that the wheel-rail force obtained as an input for the vehicle-roadbed simulation was simultaneously multiplied by the influence coefficient and used as the input to the (duplicate) track structure simulation, all done at one time on the analog computer.

For the transient analysis, the car was assumed to encounter a 1/4-inch drop in rail level (such as a severely misaligned joint) as it moved along at 50 mph. This transient analysis was done not only for a weak soil (k_o = 100 psi/in.), as in the steady-state analysis, but also for the stiff soil (k_o = 500 psi/in.). Typical response data is shown in Figure 17 for concrete-tie and Dutch "zig-zag" structures; selected data were previously shown in Table 3.

The peak car body acceleration was proportional to the overall track stiffness, being highest for the concrete tie structure (without tie pads) and lowest for the Dutch "zig-zag" track, for both weak and stiff soils. The lowest wheel-rail force was obtained on the unpadded wooden-tie "conventional track" for both weak and stiff soils. The highest wheel-rail force for a weak soil condition was on the Dutch "zig-zag" track, but for a stiff soil condition the concrete tie track had the highest force. Although the Dutch design has a low spring rate, its high mass tends to increase the wheel-rail impact force. With the soft soil, differences in the five structures gave considerably different impact forces, but with the stiffer soils the wheel-rail forces were less sensitive to the differences in the five track structures.

Further work with this simulation needs to be done, and in particular, a validation of the computer program should be made by comparing computer data with actual measured track response data. Roadbed damping should be investigated, as well as the possible need for simulating the clearance which can exist between ties and ballast, the nonlinear effect due to lack of tension in the ballast, etc.

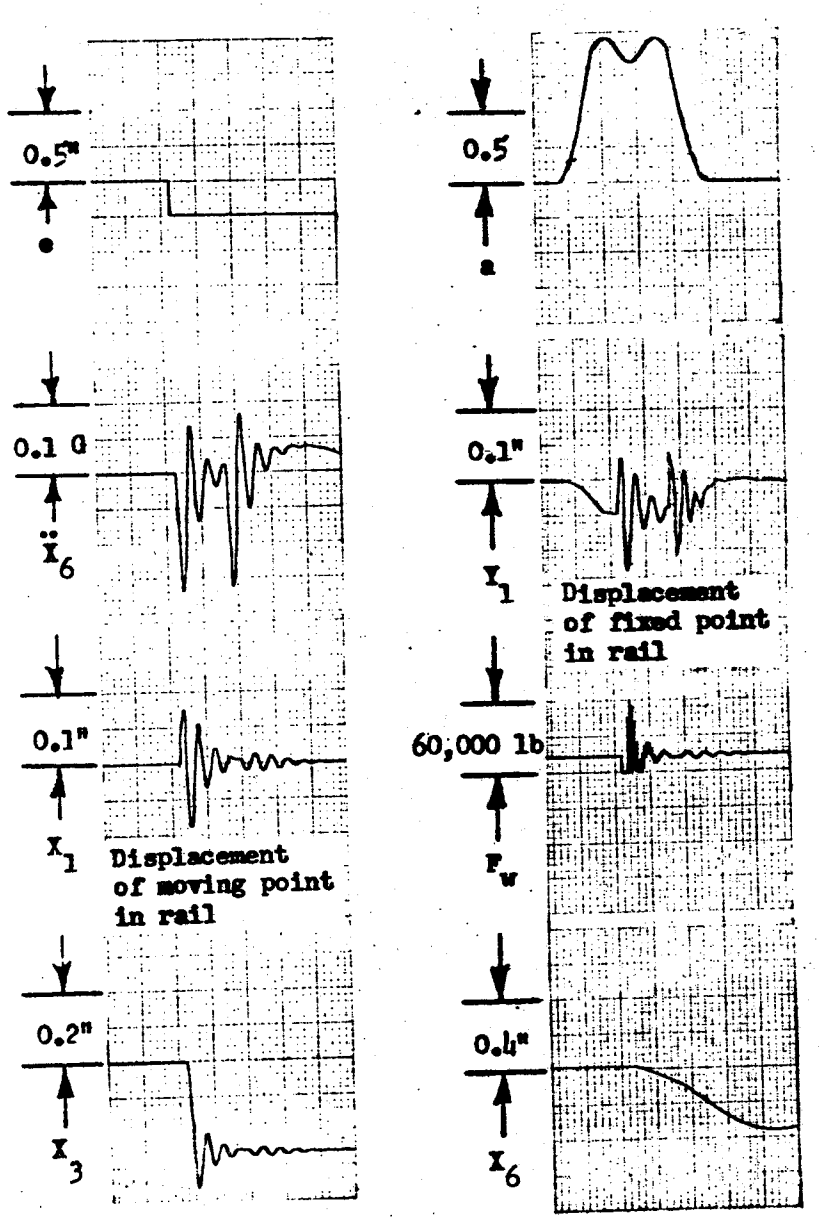

A) MR-3 Concrete ties, no pads.

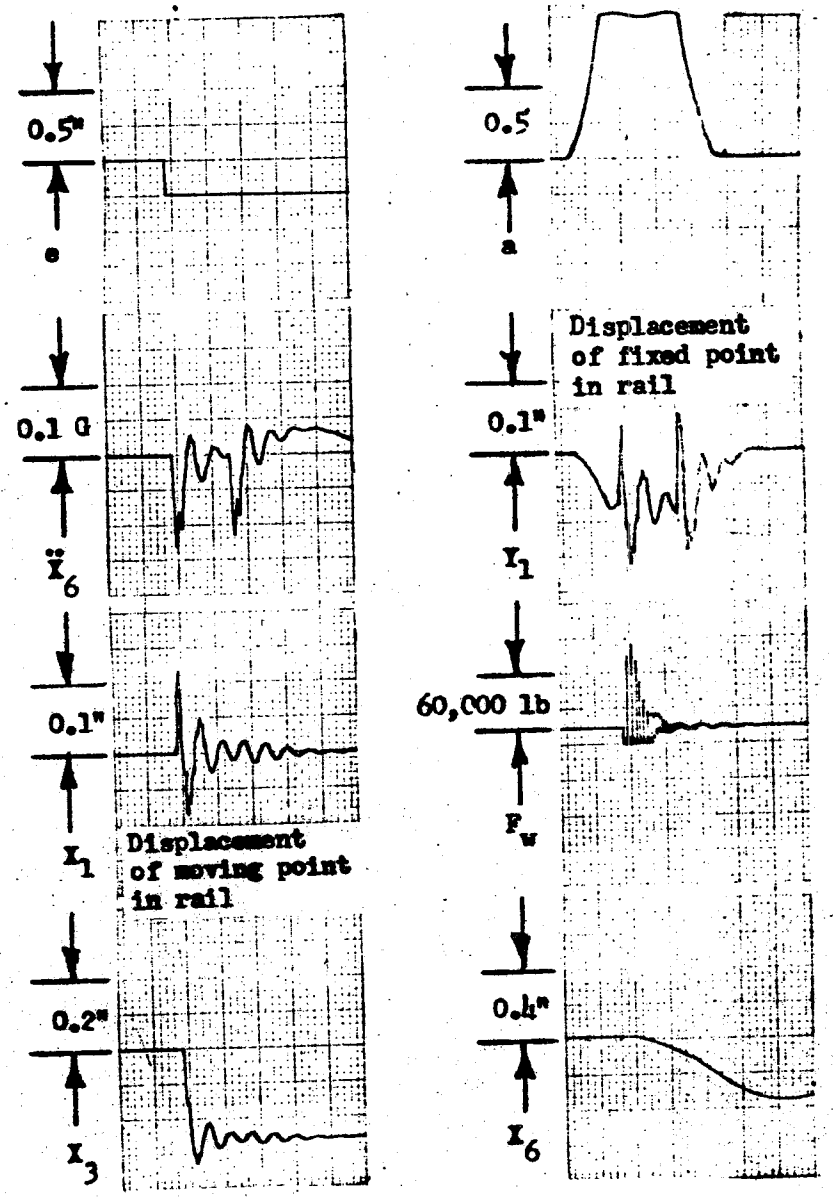

B) Dutch Zig-Zag structure.

Figure 17. Response of two tie-type track structures to step discontinuity in track profile. (Soil K_o = 100 lb/in^3).

Rail Fastener Analysis

Just as a chain is no stronger than its weakest link, the track structure can be no better than the rail fastener--composing, as it does, the vital link between rail and supporting structure. In other studies during this project the rail fastener was represented only in general form by a spring acting in the vertical direction; in this analysis it was desired to look at specific fasteners in detail and to use computer programs to aid in fastener evaluation. Unfortunately, complete data on only one fastener was obtained in time to be used in the computer analysis, but the good correlation of computer results with the manufacturer's test data demonstrated the validity of the analytical approach.

The basic function of the rail fastener is to transmit loads applied to the rail (by the train, by temperature contraction and expansion, etc.) to the supporting structure (ties, beams, etc.) without allowing any permanent motion of the rails. Although there are enough rail fastener designs on the market to make a general analysis appear formidable, the common element to all is that their contact with the rail is frictional, meaning that their holding power cannot exceed the combined frictional force exerted by all elements contacting the rail, including the rail clips and the tie pad or tie plate beneath the rail. These friction forces must prevent permanent vertical, lateral, and longitudinal rail motion.

Therefore, the basic criterion for functional effectiveness is the magnitude of this holding force and the consistency with which it is maintained during wheel passage and over long periods of time. Regardless of other attributes, this fundamental requirement must be met.

The rail displacements which occur during train passage are important to the dynamics of the train, so the vertical and lateral spring rates of the rail as restrained by the fastener are important. Furthermore, the dynamic loads transmitted into the support structure by the rail fastener are important measures of fastener performance. Other features, such as noise and

vibration isolation and electrical insulation, are desirable in many applications. If a resilient pad is used, these functional characteristics are highly dependent on the properties of the resilient pad so this is an important part of the rail fastener. Loads and stresses developed within the various fastener components and support structure are, of course, very important, in that they determine whether yielding or fatigue failure will occur, either of which means a loss of holding power.

Cost of the rail fasteners is also very important. However, during this study of fasteners, only their functional effectiveness was analyzed. No attempt was made to compare them from a cost standpoint.

Originally, four rail fasteners were chosen for analysis. These were shown in Figure 7, and are as follows:

(1) English Pandrol rail clip

(2) Swedish fist clip

(3) German Delta clip

(4) Rigid-type clips designed for American MR-3 concrete ties.

However, information for the Swedish and German fasteners required for representing them in a computer program (to determine stresses and deflections as a function of the load) was not received in time to be included in the study, and as a result a more general study of fastener design was made.

Mathematical Representation of Rail Fasteners

Although there is a wide variation in rail fasteners, most of them can be represented by the general model shown in Figure 18-A.

Combining some of the spring rates, the model shown in Figure 18-A can be reduced to that shown in Figure 18-B. There is some equivalent vertical stiffness, K_c, exhibited by the hold-down device which usually is simply the spring rate of the clip itself. The rail pad is represented by a vertical spring with rate k_p, and a torsional spring with rate K_{pt}, acting at the center of the base of the rail.

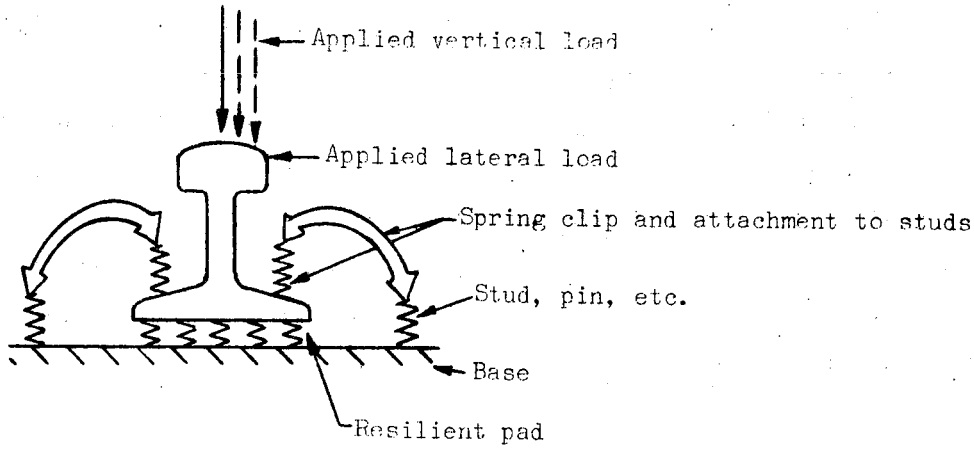

18-A

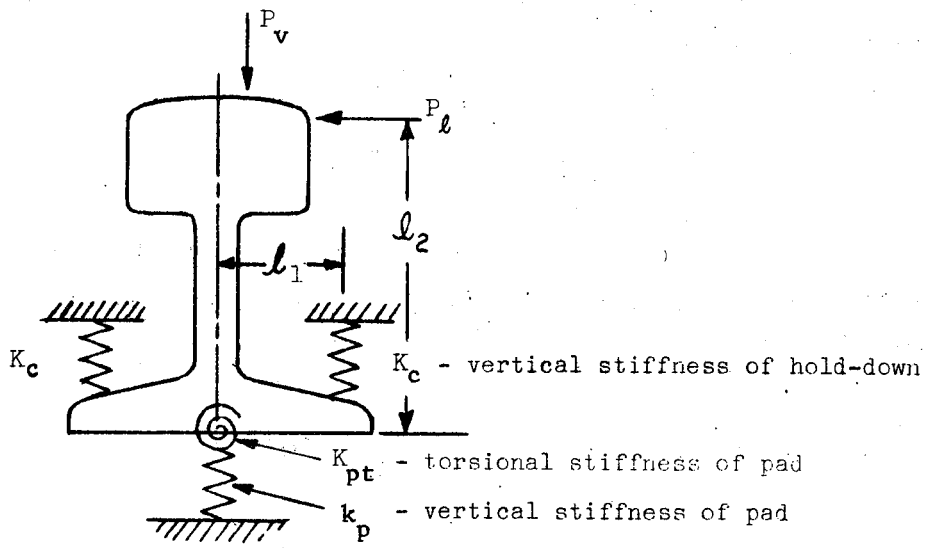

18-B

FIGURE 18. REPRESENTATION OF RAIL FASTENER FOR LOAD-DEFLECTION ANALYSIS

Since a continuous rail acts as a beam and distributes the wheel load longitudinally, the vertical load transmitted to the tie or other support is only a portion of the applied wheel load. For example, Table 5 shows that with a 22,500-pound wheel load, the tie load is around 7,000 pounds, or approximately one-third of the wheel load. This distinction must be kept in mind when discussing spring rates, and in this discussion the spring rates of an individual fastener are considered.

The fastener vertical and torsional spring rates will now be written. The vertical spring rate is equal to the sum of the two clip spring rates and the pad spring rate. Referring to Figure 18,

$$K_v = k_p + 2K_c \quad . \tag{3}$$

The deflection y for any vertical load P_v transmitted through the fastener can be written as follows:

$$y = \frac{P_v}{k_p + 2K_c} \quad . \tag{4}$$

The loss of holding force, or preload, of the two clips under an applied wheel load is equal to the vertical deflection times the spring rate of each clip times two, or

$$\Delta F_{pr} = \frac{2P_v(K_c)}{k_p + 2K_c} \quad . \tag{5}$$

Loss of frictional holding power of the clips tends to be compensated by the gain in frictional holding power of the tie plate or resilient pad as the wheel passes over. However, if a resilient pad is used and the clip preload force is completely lost, shear movement of the pad may allow permanent longitudinal motion of the rail, depending on the restraint offered by adjacent clips.

The problem of lateral load or deflection of a rail is somewhat similar to the problem of the vertical deflection of a beam on an elastic foundation, but it is complicated by a number of things. Since the lateral force is applied by the wheel flange at the head of the rail, but resisted by the fastener at the base of the rail, torsion as well as lateral displacement is involved.

The torsional deflection of the rail at the section where the wheel loads are applied is difficult to determine precisely, due to the noncircular cross section of the rail and the manner in which the torsion is applied to the rail. Lateral bending of the head and flange further complicate the problem. The torsional restraint offered by typical fasteners appears to be substantial compared with the torsional stiffness of the rail. For this reason, the torsional deflection of the rail was calculated by assuming that only one fastener resists the torsional loads introduced by the wheel. With this assumption, the calculated stresses in the fastener will be higher than in the actual case where there is some load distribution.

Considering now the torsional spring rate of the fastener, it can be shown that the torsional spring rate K_{pt}, of the resilient pad is equal to $k_p w^2/12$, where k_p is the vertical spring rate and w is the width of the pad. The torsional deflection of the rail cross section due to a lateral wheel load P_ℓ (assuming one fastener with two clips takes the full lateral load) is then

$$\eta = \frac{P_\ell \ell_2}{K_{pt} + 2\ell_1^2 K_c} , \tag{6}$$

where

η = angular deflection of rail cross section, radians

ℓ_1, ℓ_2 = distances as shown in Figure 18-B.

The vertical deflection at the clips due to the rail angular deflection is

$$y_\eta = \pm\eta\ell_1 . \tag{7}$$

The total clip deflection under combined vertical and lateral load is

$$y_t = y \pm y_\eta \quad . \tag{8}$$

Looking now at the various commercial rail fastener assemblies, data indicated that the spring rate of the clips was on the order of 3000 to 8500 lb/in. for the foreign clips and 70,000 to 100,000 lb/in. for the rigid-type clips designed for the MR-3 ties. Spring rates for the foreign clips were based on published data, while for the rigid-type clips that portion of the clip extending from the bolt centerline to the rail contact point was assumed to be a steel cantilever, 1.5 inches long, 2 inches wide, and 1/4-inch thick. The calculated spring rate for such a cantilever is 69,400 lb/in., and since some of the rigid-type clips are stiffened by flanges, the range of 70,000 to 100,000 lb/in. was not considered to be excessive.

A resilient pad vertical spring rate of 700,000 to 750,000 lb/in. was chosen, based on two factors. First, in the Phase I study the upper value was chosen as being desirable for use with the massive beam-type structures, and secondly, this value is probably on the low side of many of the commercial resilient pads now in service both here and abroad.

Using these numbers, the lateral spring rate of a section of rail held by two fasteners was calculated to be as follows:

Fastener		Installed Rail Lateral Spring Rate
English Pandrol	(K_u = 5000 lb/in.)	43,700 lb/in.
Swedish Fist	(K_u = 6000 lb/in.)	43,900 lb/in.
German Delta	(K_u = 8500 lb/in.)	44,300 lb/in.
Typical American Fastener for MR-3 Ties	(K_u = 70,000 lb/in.)	54,300 lb/in.

Note that it is the resilient pad which provides the bulk of the lateral stiffness, and large changes in clip vertical stiffness do not affect the overall lateral stiffness greatly.

To illustrate the importance of both the clip spring rates and the resilient pad spring rate on the loss of preload or holding force, calculations were made for a range of spring rates. It was assumed that 7500 pounds (one-third of a 22,500 wheel load) was transmitted through the fastener. The results are plotted in Figure 19, and show that the loss of preload or holding power increases as the clip spring rate increases, but decreases as the resilient pad spring rate decreases.

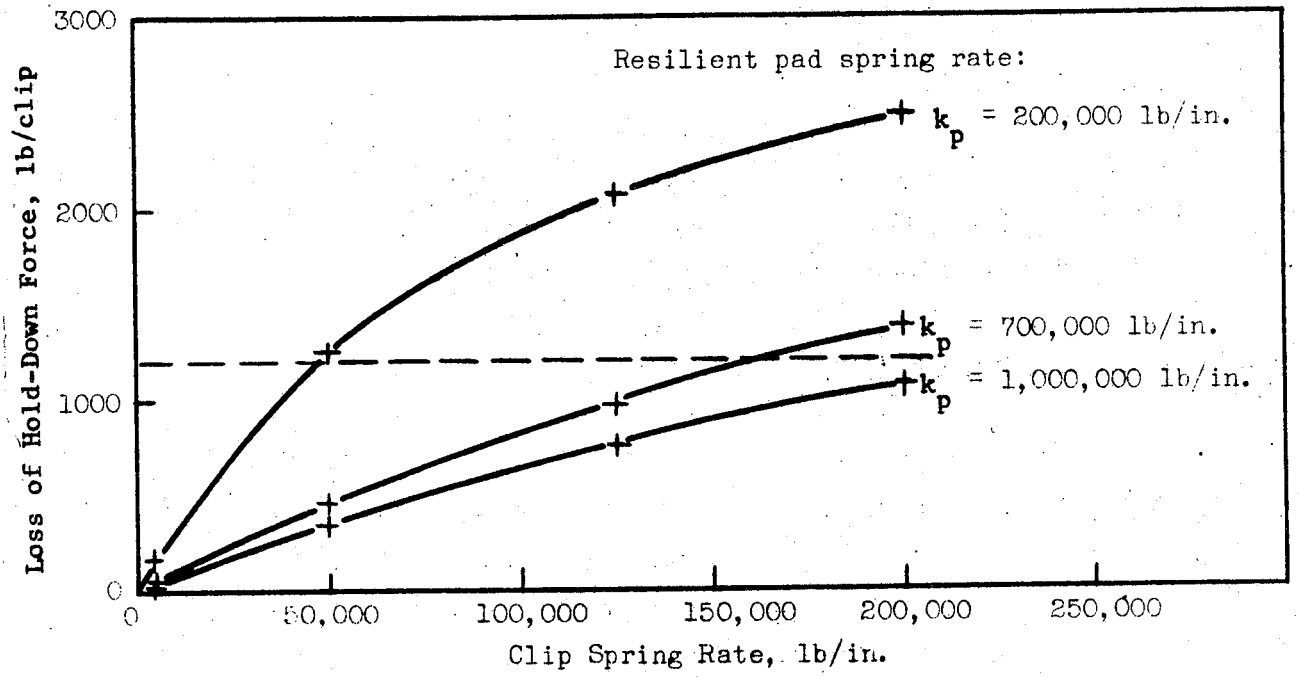

FIGURE 19. RELATIONSHIP OF CLIP HOLD-DOWN FORCE TO CLIP AND RESILIENT PAD SPRING RATES

The curves show that with a pad stiffness of 700,000 lb/in., any of the clips having spring rates of 10,000 pounds per inch or less lose very little holding power under this 22,500-pound wheel load. However, when the clip spring rate approaches 100,000 pounds per inch, the loss approaches 1,000 pounds per clip, a significant amount.

Horizontal lines could be drawn on the curve to show various preloads. For example, the dashed line shown represents a 1200-pound preload, and the figure shows that this load is completely lost with a pad stiffness of 700,000 pounds if the clip spring rate is 160,000 lb/in. or more.

Perhaps even more meaningful is a calculation of the dimensional error necessary to produce load loss. It can be assumed that eventually--if not initially--some dimensional error will exist in the load stackup. This could be produced by wear of the clip or rail at the contact point, by yielding of the clip or extension of the holddown bolt, etc. For a fairly rigid clip (100,000 lb/in.) the loss of preload due to a 1/16-inch dimensional change is (10^5) (1/16), or 6,250 pounds. This is, perhaps, the most significant point of the fastener analysis--that is, it is very difficult to maintain a constant holddown force on the rail with high spring-rate fasteners.

Pandrol Rail Clip Stress Analysis

The Pandrol rail clip was analyzed using a Battelle structural analysis digital computer program. This program is based on the stiffness matrix method. A structure (in this case the rail clip) is represented by a finite number of beam elements that can be either straight beams with or without shear deflection, or curved beams.

Figure 20 shows a sketch of the Pandrol rail clip and the node points for the finite element model. A total of fifteen beam elements including both straight and curved segments was used. An XYZ coordinate axis is shown on the sketch with the Z-axis corresponding to the vertical direction of the clip in the installed position. The node point coordinates are listed in Table 7. The clip restraints consisted of displacement restraints in the

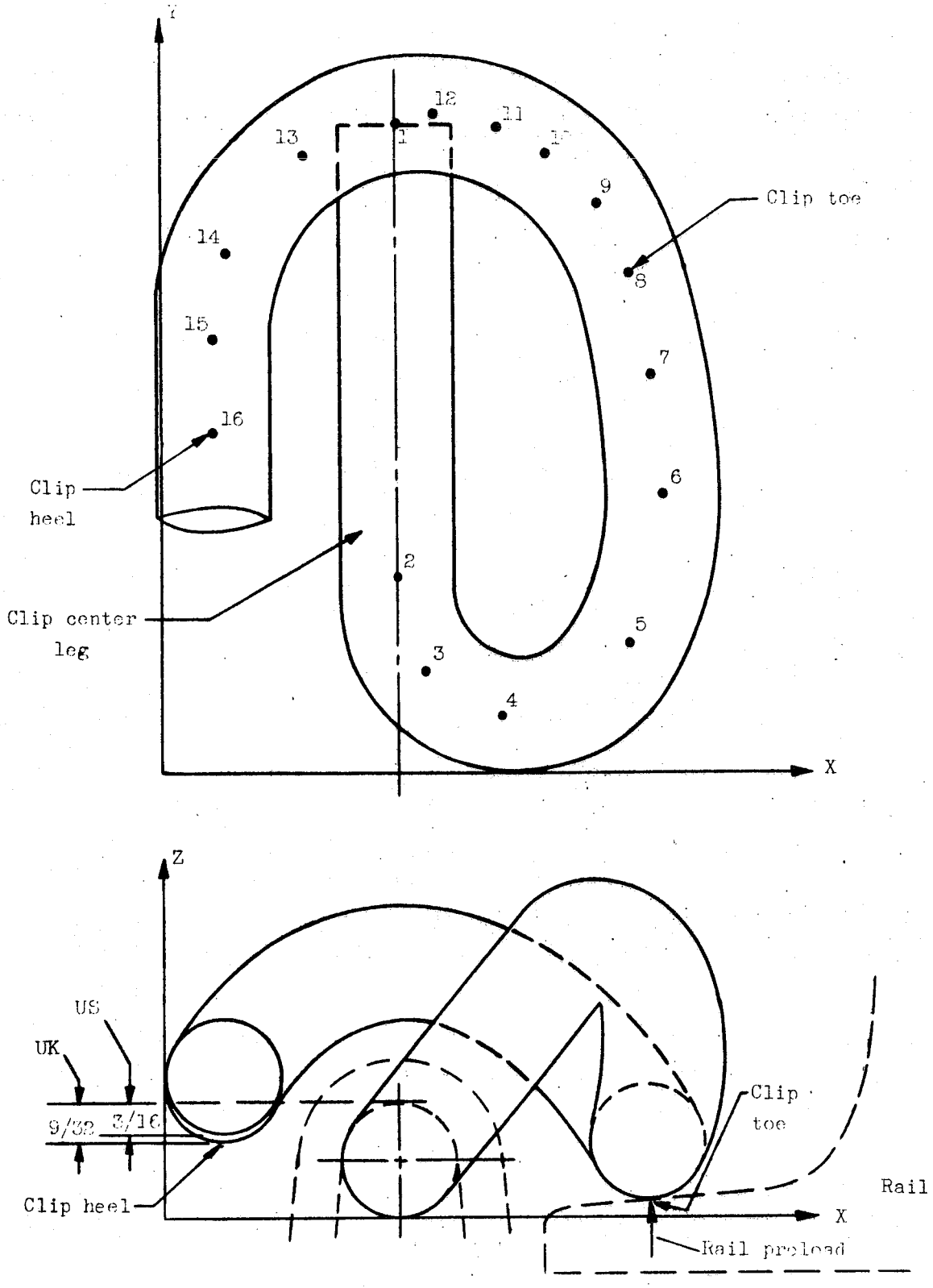

FIGURE 20. PANDROL RAIL CLIP

TABLE 7. NODE POINT COORDINATES FOR ANALYSIS MODEL OF PANDROL RAIL CLIP

Node	X, inch	Y, inch	Z, inch
1	1.65	4.55	0.40
2	1.65	1.42	0.40
3	1.82	0.73	0.63
4	2.32	0.32	1.22
5	3.23	0.90	1.92
6	3.48	1.95	1.57
7	3.44	2.75	0.76
8	3.29	3.50	0.48
9	3.20	3.98	0.76
10	2.74	4.46	1.33
11	2.32	4.52	1.60
12	1.90	4.56	1.70
13	1.11	4.25	1.63
14	0.58	3.63	1.18
15	0.38	3.03	1.04
16	0.38	2.43	0.94

X, Y, and Z directions at Nodes 1 and 2 and in the Z direction at Node 16. A vertical load of 1000 pounds was applied at Node 8, and the resulting deflections and dominant stresses were computed. These are listed in Tables 8 and 9, respectively.

At the completion of the stress analysis, a set of manufacturer's load-deflection curves was obtained from Evans Products Company. Figure 21 shows these data for both the British and United States installation configurations. The difference in the two configurations is a slight rotation of the clip about its center leg. The British assembly locates the base of the clip heel 9/32-inch below the top of the center leg. In the United States the clip is used with the base of the heel 3/16-inch below the top of the center leg.

The stress analysis model corresponds to the British configuration and the calculated toe deflection with a load of 1000 pounds was quite accurate.

However, the measured load-deflection data indicates a significant nonlinear stiffening effect so that the effective clip stiffness at the manufacturer's estimated installation load of 1550 pounds is considerably higher than that calculated using the linear analytical model. As shown in Figure 21, the measured clip stiffness is 5000 lb/in. in the vicinity of the installed load of 1550 pounds whereas the calculated stiffness from the linear analysis is 3080 lb/in.

TABLE 8. PANDROL RAIL CLIP DEFORMATION (INCHES) WITH 1000-POUND VERTICAL LOAD AT NODE 8

Node	X	Y	Z
1	0.00	0.00	0.00
2	0.00	0.00	0.00
3	-0.038	-0.002	0.023
4	-0.112	-0.009	0.082
5	-0.23	-0.026	0.212
6	-0.164	-0.013	0.287
7	-0.069	0.015	0.310
8	-0.038	0.025	0.319
9	-0.067	0.016	0.325
10	-0.129	-0.003	0.293
11	-0.157	-0.013	0.241
12	-0.173	-0.017	0.197
13	-0.166	-0.016	0.115
14	-0.113	-0.007	0.040
15	-0.095	-0.005	0.012
16	-0.087	-0.003	0.00

TABLE 9. PANDROL RAIL CLIP STRESSES WITH 1000-POUND VERTICAL LOAD AT NODE 8

Node	Maximum Shear Stress, psi	Maximum Bending Stress, psi
2	2,300	64,090
3	12,040	93,240
4	28,930	104,000
5	50,360	60,870
6	46,010	34,370
7	30,810	55,880
8	39,840	28,250
9	34,910	44,560
10	31,010	49,660
11	26,590	50,228
12	29,720	34,450
13	20,170	33,010
14	9,200	26,610
15	5,140	13,480
16	2,740	0

From a stress standpoint, the calculated stress of 156,000 psi which would be obtained from the linear computer program is quite close to measured values of 140,000 psi, quoted by the manufacturer. The location of the maximum stress found in practice and computed is also identical. Therefore, it was concluded that the computer program is an effective tool for analyzing fasteners.

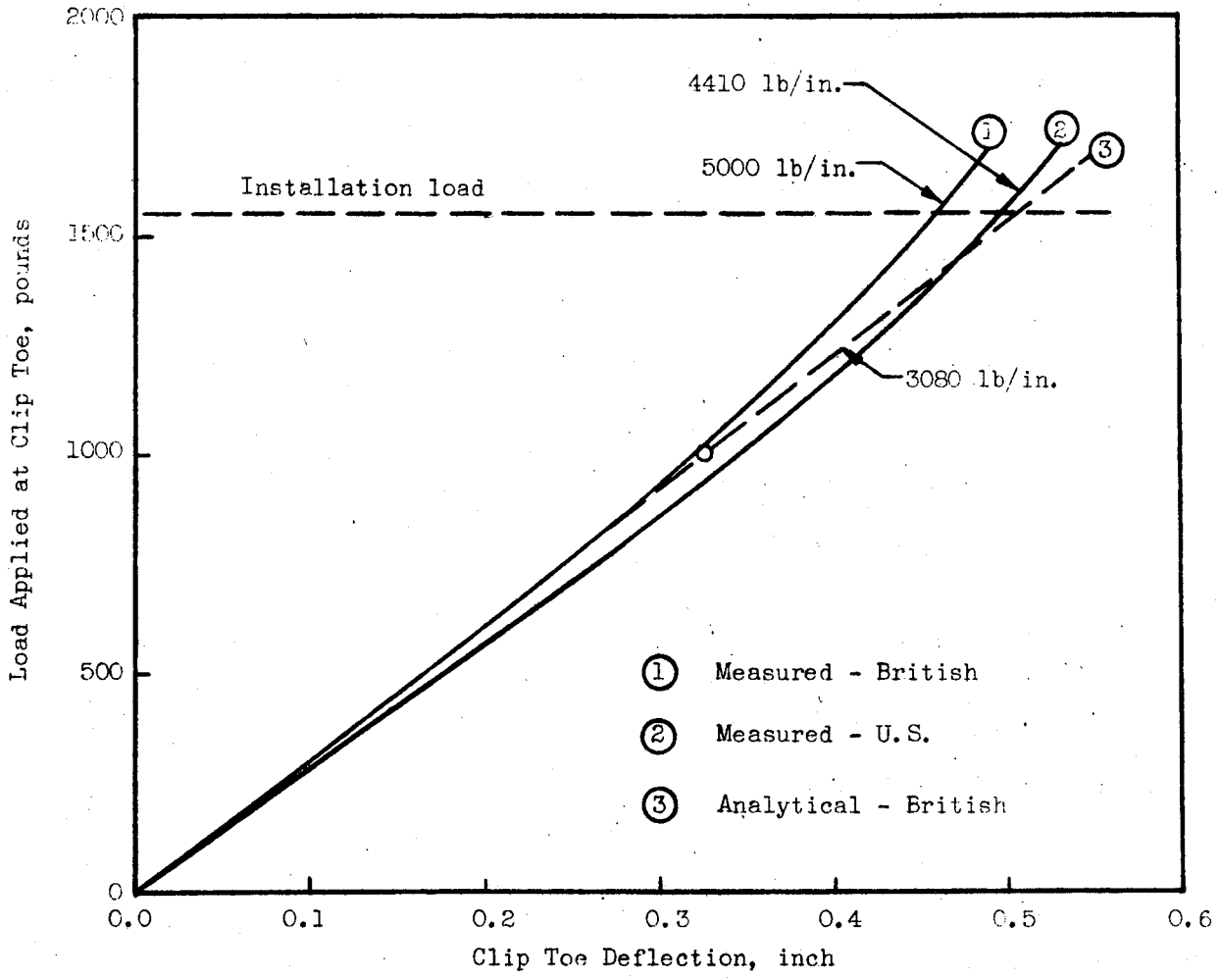

FIGURE 21. COMPARISON OF ANALYTICAL AND MEASURED LOAD-DEFLECTION DATA OF THE PANDROL RAIL CLIP